arXiv:0805.4047v1 [physics.class-ph] 27 May 2008

On Constructing the Asymptotic Solutions for Phase Transitions in a Slender Cylinder Composed of a Compressible Hyperelastic Material with Clamped End Conditions

Hui-Hui Dai[1], Jiong Wang[2] and Zhen Chen[3]

[1]Department of Mathematics and Liu Bie Ju Centre for Mathematical Sciences,
City University of Hong Kong, 83 Tat Chee Avenue, Kowloon Tong, Hong Kong
Email: mahhdai@cityu.edu.hk

[2]Department of Mathematics, City University of Hong Kong, 83 Tat Chee Avenue,
Kowloon Tong, Hong Kong
Email: jiongwang2@student.cityu.edu.hk

[3]Department of Civil and Environmental Engineering,
University of Missouri-Columbia,Columbia, MO 65211-2200, USA

Abstract

In this paper, we study phase transitions in a slender circular cylinder composed of a compressible hyperelastic material with a non-convex strain energy function. We aim to construct the asymptotic solutions based on an axisymmetrical three-dimensional setting and use the results to describe the key features (in particular, instability phenomena) observed in the experiments by others. The difficult problem of the solution bifurcations of the governing nonlinear partial differential equations (PDE's) is solved through a novel approach. By using a methodology involving coupled series-asymptotic expansions, we derive the normal form equation of the original complicated system of nonlinear PDE's. By writing the normal form equation into a first-order dynamical system and with a phase-plane analysis, we manage to deduce the global bifurcation properties and to solve the boundary-value problem analytically. The asymptotic solutions (including post-bifurcation solutions) in terms of integrals are obtained. The engineering stress-strain curve plotted from the asymptotic solutions can capture the key features of the curve measured in a few experiments (e.g., the stress drop, the stress plateau, and the small stress valley). It appears that the asymptotic solutions obtained shed certain light on the instability phenomena associated with phase transitions in a cylinder, in particular the role played by the radius-length ratio. Also, an important feature of this work is that we consider the clamped end conditions, which are more practical but rarely used in literature for phase transition problems.

Key words: Phase transformation; Hyperelastic material; Asymptotic analysis; Cylinder; Bifurcations of PDE's

1 Introduction

Applications of phase-transforming materials such as shape memory alloys (SMAs) and shape memory polymers are very broad. For example, they have been used to make satellite dampers, golf club heads and snake-like robots and so on. In particular, these materials have been used to design many minimal surgery devices (Pelton *et al.* 1997). A deep and thorough understanding of the behaviour of this type of phase-transforming material is essential in the manufacturing and designing of these devices.

Systematic experiments on uniaxial extensions of superelastic NiTi alloy (a kind of shape memory alloys and also one kind of phase-transforming materials) wires and strips (Shaw & Kyriakides 1995, 1997, 1998) showed the measured engineering stress-strain curves have the key features: The nucleation stress occurs at a local maximum which is significantly larger than the Maxwell stress; following the nucleation stress there is a sharp stress drop; and afterwards there is a stress plateau. These features were also observed in experiments done by others (Sun *et al.* 2000, Tse & Sun 2000, Favier *et al.* 2001 and Li & Sun 2002).

Theoretically, solid-solid phase transitions have also been studied for a long time in the context of both continuum and lattice theories. The seminal work of Ericksen (1975), which considered a continuum one-dimensional stress problem, made clear that for a non-convex strain energy function the solution with two phases can arise and there are multiple solutions. Based on the lattice model for a two-phase martensitic material, it is possible to deduce in the related continuum model the strain-energy function has double wells; see Ball & James (1992). In general, it is now understood that in the continuum scale for a material whose strain-energy function is non-convex phase transitions can take place (see also, Abeyaratne *et al.* 2001). With a proper choice of a strain-energy function, phase transitions can be modeled through a continuum theory. Still, to justify this point of view, it is desirable (probably necessary) to compare the analytical solutions based on this type of energy functions with experimental results. But, the difficulty is that we lack mathematical theories for mixed type equations that typically arise from non-convex energy functions. Analytical solutions for boundary-value problems are very few. In the classical paper of Ericksen (1975), analytical solutions were constructed for a static problem based on a pure one-dimensional stress model, which neglects the effect from other dimensions. However, a one-dimensional model appears to be not sophisticated enough to capture some key features observed in experiments. We give the explanations below.

In the experiments (Shaw & Kyriakides 1995, 1997; Li & Sun 2002), it was observed that after the nucleation stress was reached the nucleation process began and accompanying with it there was a radial contraction (necking). Also, after the two-phase state was formed, the deformation was inhomogeneous, one part being thin and one part being thick. As pointed out by Chang *et al.* (2006) that the axial extent of the transformation front is of the order of the radius. Thus, to model the nucleation process and the inhomogeneous deformation of different thicknesses, one should consider the radial deformation.

Theoretically, if one treats the problem as a one-dimensional stress one, there is a discontinuous interface between two phases with two different strain values. The thicknesses of the cylinder at two phases are different, thus the shear strain U_Z (U is the radial displacement and Z is the axial coordinate) is nonzero (infinite at the phase boundary). The traction-free boundary conditions require the two stress components Σ_{Rr} (depending on U_Z^2 up to the second order) and Σ_{Rz} (depending on U_Z) to be zero at the lateral surface, which cannot be satisfied. Thus, it appears that to model phase transitions by a one-dimensional stress approximation violates the traction-free boundary conditions.

In the papers of Dai & Cai (2006) and Cai & Dai (2006), phase transitions in a slender cylinder composed of a *special incompressible* elastic material was considered. A novel series-asymptotic approach is utilized to reduce the field equations. A proper asymptotic model equation is derived, which takes into account the influences of the radial deformation and traction-free boundary conditions. The solutions for two boundary-value problems are obtained, and they could capture the key features observed in experiments.

In this paper, we study the phase transitions in a slender cylinder composed of a *general compressible* elastic material due to tension/extension. Also, different from the previous studies on *incompressible* materials, here we further consider the coupling effect of the material nonlinearity and geometrical size. Another important new feature is that we consider the more practical clamped end conditions instead of the natural boundary conditions used in Cai & Dai (2006).

We consider the problem in a three-dimensional setting, different from the one-dimensional stress problem studied by Ericksen (1975). However, the strain-energy function is assumed to have the same property as that in Ericksen (1975), i.e., for a one-dimensional stress problem the stress-strain curve has a peak-valley combination (cf. figure 1). We aim at constructing the asymptotic solutions and using them to explain the experimental results.

Mathematically, to deduce the analytical solutions for the present problem is a very difficult task. One need to deal with coupled nonlinear partial differential equations (PDE's) together with complicated boundary conditions. Further, the existence of multiple solutions (corresponding to the instability phenomena (e.g., stress drop) observed in experiments) makes the problem even harder to solve. Here, the analysis is carried out by a novel methodology developed earlier (Dai & Huo 2002; Dai & Fan 2004; Dai & Cai 2006), which is capable of treating the global bifurcation problem of nonlinear PDE's and obtaining the post-bifurcation solutions. We construct the solutions and extract from them important information on the deformation configurations, the nucleation stress, the instability phenomena and the transformation front. Comparisons with experimental results are made, which show that the asymptotic solutions can capture the key features of the experimental engineering stress-strain curves and the instability phenomena as observed in experiments. The qualitative agreements give supporting evidence that a non-convex strain energy function can be used to describe solid-solid phase transitions and the instability phenomena in phase transformations are mainly due to the non-convexity of the strain energy function.

This paper is arranged as follows. In section 2, we formulate the field equations by treating the slender cylinder as a three-dimensional object. In section 3, we carry out a non-dimensionalization process to extract the important small variable and two small parameters which characterize this problem. Then we derive the normal form equation of the original governing nonlinear PDE's in section 4, through series and asymptotic expansions. In section 5, we show that the Euler-Lagrange equation can also lead to the same normal form equation, which justifies our method in deriving this equation. In section 6, we propose the clamped boundary conditions. In section 7, we construct the asymptotic solutions for both a force-controlled problem and a displacement-controlled problem. We also use the solutions obtained to explain some experimental results. Finally, some conclusions are drawn.

2 Three-dimensional field equations

We consider the axisymmetric deformations of a slender elastic cylinder subject to a static axial force at two ends. The lateral surface is traction-free and the end conditions will be considered later. In an undeformed state, the radius of the cylinder is a and the total length is $2l$. It is assumed that $\delta = a/l << 1$. We take the cylindrical polar coordinate system and denote (R, Θ, Z) and (r, θ, z) the coordinates of a material point of the cylinder in the reference and current configurations, respectively. The finite radial and axial displacements can be written as

$$U(R, Z) = r(R, Z) - R, \quad W(R, Z) = z(R, Z) - Z. \tag{2.1}$$

We introduce the orthonormal bases associated with the cylindrical coordinates and denote these by $\mathbf{E}_R$, $\mathbf{E}_\Theta$, $\mathbf{E}_Z$ and $\mathbf{e}_r$, $\mathbf{e}_\theta$, $\mathbf{e}_z$ in the reference and current configurations, respectively. Then the deformation gradient tensor $\mathbf{F}$ is given by

$$\mathbf{F} = (1+U_R)\mathbf{e}_r\otimes\mathbf{E}_R+U_Z\mathbf{e}_r\otimes\mathbf{E}_Z+(1+\frac{U}{R})\mathbf{e}_\theta\otimes\mathbf{E}_\Theta+W_R\mathbf{e}_z\otimes\mathbf{E}_R+(1+W_Z)\mathbf{e}_z\otimes\mathbf{E}_Z. \tag{2.2}$$

For an hyperelastic material, the strain energy function Φ is a function of the three invariants I_1, I_2 and I_3 of the left Cauchy-Green strain tensor $\mathbf{B} = \mathbf{F}\mathbf{F}^T$; that is, $\Phi = \Phi(I_1, I_2, I_3)$. We suppose that Φ is non-convex in a pure one-dimensional stress problem such that phase transition can take place. The nominal stress tensor $\mathbf{\Sigma}$ is given by

$$\Sigma = \frac{\partial\Phi}{\partial\mathbf{F}}, \quad \Sigma_{ji} = \frac{\partial\Phi}{\partial F_{ij}}. \tag{2.3}$$

If the strains are small, it is possible to expand the nominal stress components in term of the strains up to any order. The formula containing terms up to the third order material nonlinearity is (cf. Fu & Ogden 1999)

$$\Sigma_{ji} = a^1_{jilk}\eta_{kl} + \frac{1}{2}a^2_{jilknm}\eta_{kl}\eta_{mn} + \frac{1}{6}a^3_{jilknmqp}\eta_{kl}\eta_{mn}\eta_{pq} + O(|\eta_{st}|^4), \tag{2.4}$$

where η_{ij} is the components of the tensor $\mathbf{F}-\mathbf{I}$, a^1_{jilk}, a^2_{jilknm} and $a^3_{jilknmqp}$ are incremental elastic moduli, which can be calculated once a specific form of the strain-energy function is given, and the formulas can be found in Appendix A. From the formula (2.4), we could obtain the nominal stress components Σ_{ji}. For example,

$$\begin{aligned}\Sigma_{Zz} =&\xi_2\frac{U}{R} + \xi_1 W_Z + \xi_2 U_R + \frac{1}{2}(\eta_2\frac{U^2}{R^2} + \eta_4 U_Z^2 + 2\eta_2\frac{UW_Z}{R} + \eta_1 W_Z^2 + 2\eta_3\frac{UU_R}{R}\\ &+ 2\eta_2 W_Z U_R + \eta_2 U_R^2 + 2\eta_7 U_Z W_R + \eta_4 W_Z^2) + \frac{1}{6}(\theta_2\frac{U^3}{R^3} + 3\theta_8\frac{UU_Z^2}{R}\\ &+ 3\theta_3\frac{U^2W_Z}{R^2} + 3\theta_5 U_Z^2 W_Z + 3\theta_2\frac{UW_Z^2}{R} + \theta_1 W_Z^3 + 3\theta_4\frac{U^2U_R}{R^2} + 3\theta_7 U_Z^2 U_R\\ &+ 6\theta_4\frac{UU_RW_Z}{R} + 3\theta_2 U_R W_Z^2 + 3\theta_4\frac{UU_R^2}{R} + 3\theta_3 U_R^2 W_Z + \theta_2 U_R^3 + 6\theta_{15}\frac{UU_ZW_R}{R}\\ &+ 6\theta_{12}U_Z W_Z W_R + 6\theta_{14}U_R U_Z W_R + 3\theta_8\frac{UW_R^2}{R} + 3\theta_5 W_R^2 W_Z + 3\theta_7 U_R W_R^2),\end{aligned} \tag{2.5}$$

where ξ_i, η_j and θ_k are some elastic moduli, whose formulas are given in Appendix A. The other non-zero stress components can also be obtained but we omit their lengthy expressions for brevity. Owing to the complexity of calculations, we shall only work up to the third-order material nonlinearity. In the experiments, the maximum strain is less than 10%, and such an approximation is sufficiently accurate.

$\boldsymbol{\Sigma}$ satisfies the following field equations:

$$\mathrm{Div}(\Sigma) = 0, \tag{2.6}$$

which yields the following equations

$$\frac{\partial \Sigma_{Zz}}{\partial Z} + \frac{\partial \Sigma_{Rz}}{\partial R} + \frac{\Sigma_{Rz}}{R} = 0, \tag{2.7}$$

$$\frac{\partial \Sigma_{Rr}}{\partial R} + \frac{\partial \Sigma_{Zr}}{\partial Z} + \frac{\Sigma_{Rr} - \Sigma_{\Theta\theta}}{R} = 0. \tag{2.8}$$

We consider the case that the lateral surface of the cylinder is traction-free. Thus, we have the boundary conditions

$$\Sigma_{Rr}|_{R=a} = 0, \qquad \Sigma_{Rz}|_{R=a} = 0. \tag{2.9}$$

We shall derive the asymptotic solutions of (2.7) and (2.8) under (2.9) and some end conditions for a given external force.

Equations (2.7) and (2.8) together with (2.4) provide the governing equations for two unknowns U and W. The formal two are very complicated nonlinear partial differential equations (PDE's) and the boundary conditions (2.9) are also complicated nonlinear relations (cf. (3.3)-(3.6)). To describe the instability phenomena during phase transitions, one need to study the bifurcations of this complicated system of nonlinear PDE's. Here, we shall adopt an alternative approach involving coupled series-asymptotic expansions to tackle this bifurcation problem. A similar methodology has been developed to study nonlinear waves and phase transitions in incompressible materials (see Dai & Huo 2002, Dai & Fan 2004, Dai & Cai 2006, Cai & Dai 2006). First, we shall nondimensionalize this system to identify the relevant small variable and small parameters.

3 Non-dimensional equations

We first introduce a very important transformation

$$U = vR, \quad s = R^2, \tag{3.1}$$

then do the following scalings:

$$s = l^2\tilde{s}, \quad Z = l\tilde{z}, \quad W = h\tilde{w}, \quad v = \frac{h}{l}\tilde{v}, \quad \epsilon = \frac{h}{l}, \tag{3.2}$$

where l is the length of the cylinder, h is a characteristic axial displacement, and ϵ is regarded to be a small parameter (equivalent to a small engineering strain). Substituting (3.1) and (3.2) into (2.7) and (2.8), we obtain

$$2(\xi_2 + \xi_3)v_z + \xi_1 w_{zz} + 4\xi_3 w_s + s[2(\xi_2 + \xi_3)v_{sz} + 4\xi_3 w_{ss}] + \cdots = 0, \tag{3.3}$$

$$\xi_3 v_{zz} + 8\xi_1 v_s + 2(\xi_2 + \xi_3)w_{sz} + s4\xi_1 v_{ss} + \cdots = 0. \tag{3.4}$$

Here and hereafter,we have dropped the tilde for convenience. The full forms of (3.3) and (3.4) are very lengthy and can be found in Appendix B, here we just present the first few terms. Substituting (3.1) and (3.2) into the traction-free boundary conditions (2.9), we obtain

$$\begin{aligned}
&(\xi_1+\xi_2)v+\xi_2 w_z+s2\xi_1 v_s+\epsilon[(\frac{1}{2}\eta_1+\frac{3}{2}\eta_2)v^2+(\eta_2+\eta_3)vw_z+\frac{1}{2}\eta_2 w_z^2\\
&+s(\frac{1}{2}\eta_4 v_z^2+(2\eta_1+2\eta_2)vv_s+2\eta_2 w_z v_s+2\eta_7 v_z w_s+2\eta_4 w_s^2)+s^2 2\eta_1 v_s^2]\\
&+\epsilon^2[(\frac{1}{6}\theta_1+\frac{2}{3}\theta_2+\frac{1}{2}\theta_3)v^3+(\frac{1}{2}\theta_2+\frac{3}{2}\theta_4)v^2 w_z+(\frac{1}{2}\theta_3+\frac{1}{2}\theta_4)vw_z^2+\frac{1}{6}\theta_2 w_z^3 \qquad (3.5)\\
&+s((\frac{1}{2}\theta_5+\frac{1}{2}\theta_8)vv_z^2+\frac{1}{2}\theta_7 v_z^2 w_z+(\theta_1+2\theta_2+\theta_3)v^2 v_s+(2\theta_2+2\theta_4)vw_z v_s\\
&+\theta_3 w_z^2 v_s+(2\theta_{12}+2\theta_{15})vv_z w_s+2\theta_{14}v_z w_s w_z+(2\theta_5+2\theta_8)vw_s^2+2\theta_7 w_z w_s^2)
\end{aligned}$$

$$+s^2(\theta_5 v_z^2 v_s+(2\theta_1+2\theta_2)vv_s^2+2\theta_2 w_z v_s^2+4\theta_{12}v_s v_z w_s+4\theta_5 v_s w_s^2)+s^3\frac{4}{3}\theta_1 v_s^3]|_{s=\nu}=0,$$

$$\begin{aligned}
&\xi_3 v_z+2\xi_3 w_s+\epsilon[(\eta_7+\eta_8)vv_z+\eta_7 v_z w_z+(2\eta_4+2\eta_5)vw_s+2\eta_4 w_z w_s\\
&+s(2\eta_7 v_z v_s+4\eta_4 v_s w_s)]+\epsilon^2[(\frac{1}{2}\theta_{12}+\frac{1}{2}\theta_{13}+\theta_{15})v^2 v_z+(\theta_{14}+\theta_{15})vv_z w_z\\
&+\frac{1}{2}\theta_{12}v_z w_z^2+(\theta_5+\theta_6+2\theta_8)v^2 w_s+(2\theta_7+2\theta_8)vw_z w_s+\theta_5 w_z^2 w_s \qquad (3.6)\\
&+s(\frac{1}{6}\theta_{16}v_z^3+(2\theta_{12}+2\theta_{15})vv_z v_s+2\theta_{14}v_z w_z v_s+\theta_{17}v_z^2 w_s+(4\theta_5+4\theta_8)vv_s w_s\\
&+4\theta_7 w_z v_s w_s+2\theta_{16}v_z w_s^2+\frac{4}{3}\theta_9 w_s^3)+s^2(2\theta_{12}v_z v_s^2+4\theta_5 v_s^2 w_s)]|_{s=\nu}=0,
\end{aligned}$$

where $\nu = a^2/l^2$ (square of the diameter-length ratio) is a small parameter for a slender cylinder. We note that in the above equations the dependence on R and a/l is entirely through $s = R^2/l^2$ and $\nu = a^2/l^2$, respectively.

Equations (3.3)-(3.6) comprise a new system of complicated nonlinear PDE's with complicated boundary conditions, which is still very difficult to solve directly. However, it is characterized by a small variable s ($0 \le s \le \nu$) and two small parameters ϵ and ν, which permit us to use expansion methods to proceed further.

4 Coupled series-asymptotic expansions

From equations (3.3)-(3.6), we can see that the two unknowns w and v depend on the variable z and the small variable s and the small parameters ϵ and ν; that is

$$w = w(z, s; \epsilon, \nu), \qquad v = v(z, s; \epsilon, \nu). \tag{4.1}$$

To go further, we seek series expansions in terms of the small variable s:

$$v(z, s; \epsilon, \nu) = V_0(z; \epsilon, \nu) + sV_1(z; \epsilon, \nu) + s^2V_2(z; \epsilon, \nu) + \cdots , \tag{4.2}$$

$$w(z, s; \epsilon, \nu) = W_0(z; \epsilon, \nu) + sW_1(z; \epsilon, \nu) + s^2W_2(z; \epsilon, \nu) + \cdots . \tag{4.3}$$

Substituting (4.2) and (4.3) into (3.3), the left hand becomes a series in s and all the coefficients of s^n (n=0, 1, 2, $\cdots$) should vanish. Equating the coefficients of s^0 and s^1 to be zero yields that

$$\begin{aligned}
&4\xi_4W_1 + (2\xi_2 + 2\xi_3)V_{0z} + \xi_1W_{0zz} + \epsilon((4\eta_4 + 4\eta_5)V_0W_1 \\
&+ (2\eta_2 + 2\eta_3 + 2\eta_7 + 2\eta_8)V_0V_{0z} + 4\eta_4W_1W_{0z} + (2\eta_2 + 2\eta_7)V_{0z}W_{0Z} \\
&+ 2\eta_2V_0W_{0zz} + \eta_1W_{0z}W_{0zz}) + \epsilon^2H_1(V_0, W_0, W_1) = 0,
\end{aligned} \tag{4.4}$$

$$\begin{aligned}
&16\xi_3W_2 + (4\xi_2 + 4\xi_3)V_{1z} + \xi_1W_{1zz} + \epsilon((24\eta_4 + 8\eta_5)V_1W_1 \\
&+ (16\eta_4 + 16\eta_5)V_0W_2 + (4\eta_2 + 4\eta_3 + 12\eta_7 + 4\eta_8)V_1V_{0z} \\
&+ (4\eta_2 + 4\eta_3 + 4\eta_7 + 4\eta_8)V_0V_{1z} + 16\eta_4W_2W_{0z} + (4\eta_2 + 4\eta_7)V_{1z}W_{0z} \\
&+ 12\eta_4W_1W_{1z} + (2\eta_2 + 6\eta_7)V_{0z}W_{1z} + 2\eta_7W_1V_{0zz} + \eta_4V_{0z}V_{0zz} \\
&+ 4\eta_2V_1W_{0zz} + \eta_1W_{1z}W_{0zz} + 2\eta_2V_0W_{1zz} + \eta_1W_{0z}W_{1zz}) \\
&+ \epsilon^2H_2(V_0, V_1, W_0, W_1, W_2) = 0.
\end{aligned} \tag{4.5}$$

Similarly, substituting equations (4.2) and (4.3) into (3.4) and equating the coefficient of s^0 to be zero yields that

$$\begin{aligned}
&8\xi_1 V_1 + (2\xi_2 + 2\xi_3)W_{1z} + \xi_3 V_{0zz} + \epsilon((8\eta_1 + 8\eta_2)V_0 V_1 \\
&+ (6\eta_4 - 2\eta_5)W_1^2 + 8\eta_7 W_1 V_{0z} + (\frac{5}{2}\eta_4 + \frac{1}{2}\eta_5)V_{0z}^2 \\
&+ 8\eta_2 V_1 W_{0z} + (2\eta_2 + 2\eta_3 + 2\eta_7 + 2\eta_8)V_0 W_{1z} + (2\eta_2 + 2\eta_7)W_{0z}W_{1z} \\
&+ (\eta_4 + \eta_5)V_0 V_{0zz} + \eta_4 W_{0z}V_{0zz} + 2\eta_7 W_1 W_{0zz} + \eta_4 V_{0z}W_{0zz}) \\
&+ \epsilon^2 H_3(V_0, V_1, W_0, W_1) = 0.
\end{aligned} \tag{4.6}$$

The expressions of H_1, H_2 and H_3 are very lengthy, which are omitted for brevity. Substituting (4.2) and (4.3) into the traction-free boundary conditions (3.5) and (3.6), we obtain

$$\begin{aligned}
&(\xi_1 + \xi_2)V_0 + \xi_2 W_{0z} + \nu((3\xi_1 + \xi_2)V_1 + \xi_2 W_{1z}) + \epsilon((\frac{1}{2}\eta_1 + \frac{3}{2}\eta_2)V_0^2 \\
&+ (\eta_2 + \eta_3)V_0 W_{0z} + \frac{1}{2}\eta_2 W_{0z}^2) + \epsilon^2 H_4(V_0, W_0) + \epsilon\nu H_5(V_0, V_1, W_0, W_1) = 0,
\end{aligned} \tag{4.7}$$

$$\begin{aligned}
&2\xi_3 W_1 + \xi_3 V_{0z} + \nu(4\xi_3 W_2 + \xi_3 V_{1z}) + \epsilon((2\eta_4 + 2\eta_5)V_0 W_1 + (\eta_7 + \eta_8)V_0 V_{0z} \\
&+ 2\eta_4 W_1 W_{0z} + \eta_7 V_{0z}W_{0z}) + \epsilon^2 H_6(V_0, W_0, W_1) + \epsilon\nu H_7(V_0, V_1, W_0, W_1, W_2) = 0,
\end{aligned} \tag{4.8}$$

where the lengthy expressions for H_4-H_7 are omitted, and interested readers can find the expressions for H_i ($i = 1, \cdots, 7$) in Appendix C. In obtaining the above equations, we have neglected terms higher than $O(\epsilon\nu, \epsilon^2)$.

Now the governing equations (3.3)-(3.4) are changed into a one-dimensional system of differential equations (4.4)-(4.8) for the unknowns W_0, W_1, W_2, V_0 and V_1. By using a regular perturbation method, we can express W_1 by W_0 and V_0 from (4.4), then substitute W_1 into (4.6), we can also express V_1 by W_0 and V_0. Similarly, we substitute W_1 and V_1 into (4.5) to obtain the expression of W_2 in terms of W_0

and V_0 through the regular perturbation method. The results are given below:

$$\begin{aligned} W_1 =&(-\frac{1}{2}-\frac{\xi_2}{2\xi_3})V_{0z}-\frac{\xi_1}{4\xi_3}W_{0zz}+\epsilon(a_1V_0V_{0z}+a_2V_{0z}W_{0z}\\ &+a_3V_{0z}W_{0zz}+a_4W_{0z}W_{0zz})+\epsilon^2(a_5V_0^2V_{0z}+a_6V_0V_{0z}W_{0z}\\ &+a_7V_{0z}W_{0z}^2+a_8V_0^2W_{0zz}+a_9V_0W_{0z}W_{0zz}+a_{10}W0z^2W_{0zz}), \end{aligned} \tag{4.9}$$

$$\begin{aligned} V_1 =&(\frac{\xi_2}{4\xi_1}+\frac{\xi_2^2}{8\xi_1\xi_3})V_{0zz}+(\frac{1}{16}+\frac{\xi_2}{16\xi_3})W_{0zzz}+\epsilon(a_{11}V_{0z}^2+a12V_0V_{0zz}\\ &+a_{13}W_{0z}V_{0zz}+a_{14}V_{0z}W_{0zz}+a_{15}W_{0zz}^2+a_{16}V_0W_{0zzz}+a_{17}W_{0z}W_{0zzz})\\ &+\epsilon^2(a_{18}V_0V_{0z}^2+a_{19}V_{0z}^2W_{0z}+a_{20}V_0^2V_{0zz}+a_{21}V_0W_{0z}V_{0zz}\\ &+a_{22}W_{0z}^2V_{0zz}+a_{23}V_0V_{0z}W_{0zz}+a_{24}V_{0z}W_{0z}W_{0zz}+a_{25}V_0W_{0zz}^2\\ &+a_{26}W_{0z}W_{0zz}^2+a_{27}V_0^2W_{0zzz}+a_{28}V_0W_{0z}W_{0zzz}+a_{29}W_{0z}^2W_{0zzz}), \end{aligned} \tag{4.10}$$

$$\begin{aligned} W_2 =&(-\frac{\xi_2}{16\xi_1}+\frac{\xi_1\xi_2}{32\xi_3^2}-\frac{\xi_2^3}{32\xi_1\xi_3^2}+\frac{\xi_1}{32\xi_3}-\frac{3\xi_2^2}{32\xi_1\xi_3})V_{0zzz}+(-\frac{1}{64}+\frac{\xi_1^2}{64\xi_3^2}\\ &-\frac{\xi_2^2}{64\xi_3^2}-\frac{\xi_2}{32\xi_3})W_{0zzzz}+\epsilon(a_{30}V_{0z}V_{0zz}+a_{31}V_{0zz}W_{0zz}+a_{32}V_0V_{0zzz}\\ &+a_{33}W_{0z}V_{0zzz}+a_{34}V_{0z}W_{0zzz}+a_{35}W_{0zz}W_{0zzz}+a_{36}V_0W_{0zzzz}+a_{37}W_{0z}W_{0zzzz})\\ &+\epsilon^2(a_{38}V_{0z}^3+a_{39}V_0V_{0z}V_{0zz}+a_{40}V_{0z}W_{0z}V_{0zz}+a_{41}V_{0z}^2W_{0zz}+a_{42}V_0V_{0zz}W_{0zz}\\ &+a_{43}W_{0z}V_{0zz}W_{0zz}+a_{44}V_{0z}W_{0zz}^2+a_{45}W_{0zz}^3+a_{46}V_0^2V_{0zzz}+a_{47}V_0W_{0z}V_{0zzz}\\ &+a_{48}W_{0z}^2V_{0zzz}+a_{49}V_0V_{0z}W_{0zzz}+a_{50}V_{0z}W_{0z}W_{0zzz}+a_{51}V_0W_{0zz}W_{0zzz}\\ &+a_{52}W_{0z}W_{0zz}W_{0zzz}+a_{53}V_0^2W_{0zzzz}+a_{54}V_0W_{0z}W_{0zzzz}+a_{55}W_{0z}^2W_{0zzzz}), \end{aligned} \tag{4.11}$$

where a_i ($i = 1, 2, \cdots, 55$) are constants related to material constants, whose expressions are omitted for brevity. Substituting W_1, V_1 and W_2 into (4.7) and (4.8) and omitting the higher order terms yield the following two equations with only two unknowns W_0 and V_0:

$$\begin{aligned}&(\xi_1+\xi_2)V_0+\xi_2W_{0z}+\epsilon(b_1V_0^2+b_2V_0W_{0z}+b_3W_{0z}^2)+\epsilon^2(b_4V_0^3+b_5V_0^2W_{0z}\\&+b_6V_0W_{0z}^2+b_7W_{0z}^3)+\nu(b_8V_{0zz}+b_9W_{0zzz})+\epsilon\nu(b_{10}V_{0z}^2+b_{11}V_0V_{0zz}\\&+b_{12}W_{0z}V_{0zz}+b_{13}V_{0z}W_{0zz}+b_{14}W_{0zz}^2+b_{15}V_0W_{0zzz}+b_{16}W_{0z}W_{0zzz})=0,\end{aligned}\tag{4.12}$$

and

$$\begin{aligned}&-\xi_2V_{0z}-\frac{\xi_1}{2}W_{0zz}+\epsilon(b_{17}V_0V_{0z}+b_{18}V_{0z}W_{0z}+b_{19}V_0W_{0zz}+b_{20}W_{0z}W_{0zz})\\&+\epsilon^2(b_{21}V_0^2V_{0z}+b_{22}V_0V_{0z}W_{0z}+b_{23}V_{0z}W_{0z}^2+b_{24}V_0^2W_{0zz}+b_{25}V_0W_{0z}W_{0zz}\\&+b_{26}W_{0z}^2W_{0zz})+\nu(b_{27}V_{0zzz}+b_{28}W_{0zzzz})+\epsilon\nu(b_{29}V_{0z}V_{0zz}+b_{30}V_{0zz}W_{0zz}\\&+b_{31}V_0V_{0zzz}+b_{32}W_{0z}V_{0zzz}+b_{33}V_{0z}W_{0zzz}+b_{34}W_{0zz}W_{0zzz}+b_{35}V_0W_{0zzzz}\\&+b_{36}W_{0z}W_{0zzzz})=0,\end{aligned}\tag{4.13}$$

where b_i $(i=1,2,\cdots,36)$ are also constants related to material constants, whose expressions are omitted for brevity. (Note: Interested readers can contact the corresponding author for the formulas for a_i and b_i.) By using the above two equations, we can express V_0 in terms of W_0 and its derivatives with respect to z. From (4.12), we have

$$\begin{aligned}V_0=&\frac{-1}{\xi_1+\xi_2}[\xi_2W_{0z}+\epsilon(b_1V_0^2+b_2V_0W_{0z}+b_3W_{0z}^2)+\epsilon^2(b_4V_0^3+b_5V_0^2W_{0z}\\&+b_6V_0W_{0z}^2+b_7W_{0z}^3)+\nu(b_8V_{0zz}+b_9W_{0zzz})+\epsilon\nu(b_{10}V_{0z}^2+b_{11}V_0V_{0zz}\\&+b_{12}W_{0z}V_{0zz}+b_{13}V_{0z}W_{0zz}+b_{14}W_{0zz}^2+b_{15}V_0W_{0zzz}+b_{16}W_{0z}W_{0zzz})].\end{aligned}\tag{4.14}$$

From (4.12) and (4.13), we also have

$$V_0=\frac{-1}{\xi_1+\xi_2}[\xi_2W_{0z}+\epsilon(b_1V_0^2+b_2V_0W_{0z}+b_3W_{0z}^2)+\nu(b_8V_{0zz}+b_9W_{0zzz})]+\cdots,\tag{4.15}$$

and

$$V_{0z} = \frac{1}{\xi_2}[-\frac{\xi_1}{2}W_{0zz}+\epsilon(b_{17}V_0V_{0z}+b_{18}V_{0z}W_{0z}+b_{19}V_0W_{0zz}+b_{20}W_{0z}W_{0zz})]+\cdots . \tag{4.16}$$

Substituting $V_0 = \frac{-\xi_2}{\xi_1+\xi_2}W_{0z} + \cdots$ into (4.15) and (4.16), then substituting (4.16) into $\nu(b_8V_{0zz} + b_9W_{0zzz})$ of (4.14) and (4.15) into the other part of (4.14), we obtain

$$\begin{aligned} V_0 = &- \frac{\xi_2}{\xi_1+\xi_2}W_{0z} + \nu\frac{\xi_2-\xi_1}{16(\xi_1+\xi_2)}W_{0zzz} + \epsilon\alpha_1W_{0z}^2 + \epsilon^2\alpha_2W_{0z}^3 \\ &+ \epsilon\nu(\alpha_3W_{0zz}^2 + \alpha_4W_{0z}W_{0zzz}), \end{aligned} \tag{4.17}$$

where

$$\begin{aligned} \alpha_1 = &- \frac{\xi_1^2\eta_2 + \xi_2^2(\eta_1+2\eta_2-2\eta_3) - 2\xi_1\xi_2\eta_3}{2(\xi_1+\xi_2)^3}. \\ \alpha_2 = &\frac{1}{6(\xi_1+\xi_2)^5}[\xi_1^3(3\eta_2^2+3\eta_2\eta_3-\xi_1\theta_2) + 3\xi_1\xi_2^2(2\eta_2^2+4\eta_2\eta_3-4\eta_3^2 \\ &+ \eta_1(\eta_2+3\eta_3) - 3\xi_1\theta_2 + 3\xi_1\theta_3) + \xi_2^4(\theta_1+6\theta_3-6\theta_4) + \xi_2^3(-3\eta_1^2 \\ &- 12\eta_1\eta_2 - 12\eta_2^2 + 9\eta_1\eta_3 + 18\eta_2\eta_3 - 6\eta_3^2 + \xi_1\theta_1 - 6\xi_1\theta_2 + 12\xi_1\theta_3 \end{aligned}$$

$$\begin{aligned} &- 9\xi_1\theta_4) - \xi_1^2\xi_2(3\eta_1\eta_2 + 6\eta_2^2 + 3\eta_2\eta_3 + 6\eta_3^2 + 4\xi_1\theta_2 - 3\xi_1\theta_3 - 3\xi_1\theta_4)], \\ \alpha_3 = &\frac{1}{64\xi_1(\xi_1+\xi_2)^3}[13\xi_1^4 + 4\xi_2^3(4\eta_1-3\eta_2) - \xi_1^2\xi_2(23\xi_2+\eta_1+13\eta_2-26\eta_3) \\ &+ 4\xi_1\xi_2^2(3\eta_1-10\eta_2+4\eta_3) + \xi_1^3(10\xi_2-3\eta_1-7\eta_2+6\eta_3)], \\ \alpha_4 = &\frac{1}{16\xi_1(\xi_1-\xi_2)(\xi_1+\xi_2)^4}[3\xi_1^6 + 2\xi_2^5(-\eta_1+\eta_2) + \xi_1^3\xi_2^2(-51\xi_2+10\eta_2-6\eta_3) \\ &+ \xi_1^4\xi_2(-21\xi_2-5\eta_1+\eta_2-4\eta_3) + \xi_1^2\xi_2^3(-30\xi_2+7\eta_1+21\eta_2-4\eta_3) \\ &+ \xi_1^5(3\xi_2-\eta_1+5\eta_2+2\eta_3) - \xi_1\xi_2^4(7\eta_1+15\eta_2+4\eta_3)]. \end{aligned}$$

By substituting (4.16) and (4.17) into (4.13), we obtain

$$\begin{aligned} &W_{0zz} - \frac{1}{4}\nu W_{0zzzz} + 3\epsilon^2 D_2 W_{0z}^2 W_{0zz} \\ &+ \epsilon(2D_1 W_{0z} W_{0zz} + \nu(4D_3 W_{0zz} W_{0zzz} + 2D_3 W_{0z} W_{0zzzz})) = 0, \end{aligned} \tag{4.18}$$

where

$$\begin{aligned} D_1 =& \frac{1}{2(\xi_1+\xi_2)^2(\xi_1^2+\xi_1\xi_2-2\xi_2^2)}[\xi_1^3\eta_1 + 3\xi_1^2\xi_2(\eta_1-2\eta_2) - \xi_2^3(\eta_1+6\eta_2-6\eta_3) \\ &+ 3\xi_1\xi_2^2(\eta_1-2\eta_2+2\eta_3)], \end{aligned} \tag{4.19}$$

$$\begin{aligned} D_2 =& \frac{1}{6(\xi_1+\xi_2)^4(\xi_1^2+\xi_1\xi_2-2\xi_2^2)}[\xi_1^4(-6\eta_2^2+\xi_1\theta_1) + \xi_1^3\xi_2(24\eta_2\eta_3+5\xi_1\theta_1 \\ &- 8\xi_1\theta_2) + \xi_2^5(3\theta_1-8\theta_2+18\theta_3-12\theta_4) + 2\xi_1^2\xi_2^2(-6\eta_1\eta_2-12\eta_2^2+12\eta_2\eta_3 \\ &- 12\eta_3^3+5\xi_1\theta_1-16\xi_1\theta_2+6\xi_1\theta_3+6\xi_1\theta_4) + 2\xi_1\xi_2^3(12\eta_1\eta_3+24\eta_2\eta_3 \\ &- 24\eta_3^2+5\xi_1\theta_1-28\xi_1\theta_2+18\xi_1\theta_3+6\xi_1\theta_4) - \xi_2^4(6\eta_1^2+24\eta_2^2+24\eta_1\eta_2 \\ &- 24\eta_1\eta_3-48\eta_2\eta_3+24\eta_3^2-7\xi_1\theta_1+40\xi_1\theta_2-42\xi_1\theta_3+12\xi_1\theta_4)], \end{aligned} \tag{4.20}$$

$$\begin{aligned} D_3 =& \frac{1}{8(\xi_1-\xi_2)(\xi_1+\xi_2)^3}[2\xi_1^4+\xi_1^3(4\xi_2-\eta_1-3\eta_2)+\xi_1\xi_2^2(-4\xi_2-7\eta_1+3\eta_2) \\ &+ 6\xi_2^3(\eta_2-\eta_3) - 2\xi_1^2\xi_2(\xi_2+2\eta_1-3\eta_2-3\eta_3)]. \end{aligned} \tag{4.21}$$

Integrating (4.18) once, we obtain

$$\epsilon W_{0z} - \frac{1}{4}\epsilon\nu W_{0zzz} + \epsilon^2 D_1 W_{0z}^2 + \epsilon^3 D_2 W_{0z}^3 + \epsilon^2\nu(D_3 W_{0zz}^2 + 2D_3 W_{0z} W_{0zzz}) = A, \tag{4.22}$$

where A is the integration constant. It is important to find the physical meaning of A, since to capture the instability phenomena observed in the experiments, one needs to study the global bifurcation as the physical parameters vary. For that purpose, we consider the resultant force T acting on the material cross-section that is planar and perpendicular to the cylinder axis in the reference configuration, and the formula is

$$T = \int_0^{2\pi} \int_0^a \Sigma_{Zz} R dR d\theta. \tag{4.23}$$

By using (4.2), (4.3) and the expressions of V_0, V_1 and W_1 in terms of W_0 in (2.5), it is possible to express Σ_{Zz} in terms of W_0. Then, carrying out the integration in (4.23), we find that

$$T = \pi a^2 E[\epsilon W_{0z} - \frac{1}{4}\epsilon\nu W_{0zzz} + \epsilon^2 D_1 W_{0z}^2 + \epsilon^3 D_2 W_{0z}^3 + \epsilon^2 \nu (D_3 W_{0zz}^2 + 2D_3 W_{0z} W_{0zzz})], \tag{4.24}$$

where $E = \frac{\xi_1^2+\xi_1\xi_2-2\xi_2^2}{\xi_1+\xi_2}$ is the Young's modulus. Comparing (4.22) and (4.24), we have $A = \frac{T}{\pi a^2 E}$. If we retain the original dimensional variable and let $V = W_{0Z} = \epsilon\widetilde{w}_{0z}$, we have

$$V + D_1 V^2 + D_2 V^3 + a^2(-\frac{1}{4}V_{ZZ} + D_3 V_Z^2 + 2D_3 V V_{ZZ}) = \gamma, \tag{4.25}$$

where $\gamma = \frac{T}{\pi a^2 E}$ is the dimensionless engineering stress. Since (4.25) is derived from the three-dimensional field equations, once its solution is found, the three-dimensional strain and stress fields can also be found. Also, it contains all the required terms to yield the leading-order behavior of the original system. Therefore, we refer (4.25) as the normal form equation of the system of nonlinear PDE's (3.3) and (3.4) together with the boundary conditions (3.5) and (3.6) under a given axial resultant.

Remark: Although the final form of the normal form equation is one dimensional, it is different from other one-dimensional phenomenological models in literature (see Coleman 1983, Tong *et al.* 2001, Shaw 2002, Chang *et al.* 2006) in the sense that it is derived from the three-dimensional field equations in a mathematically consistent manner and all three-dimensional quantities can be calculated once its solutions are found. Thus, we can provide the three-dimensional current configuration in a two-phase state, which cannot be deduced in the existing one-dimensional models in literature. This equation contains a higher-order derivative term which plays the role of regularization. Trunskinovsky (1982, 1985) pioneered the idea of the regularization augmentation for solid-solid phase transitions which involves adding terms (like a strain gradient) into the usual constitutive stress-strain relation (for the gradient approach, see also Aifantis & Serrin 1983 and Triantafyllidis & Aifantis 1986). Different from these gradient theories, the gradient term (which represents the influence of the radial deformation and traction-free boundary conditions) in our equation is derived and its coefficient is explicitly given.

5 The Euler-Lagrange equation

The normal form equation (4.25) is derived in the previous section based on the equilibrium equations (2.7) and (2.8). Now, we consider the energy and show that the same equation can be derived through the variational principle. The calculations are tremendously complicated in the present method (we use Mathematica for all the symbolic computations), and if the two derivations of the normal form equation agree with each other, it also supports the correctness of our calculations.

We expand the strain energy function up to the fourth-order nonlinearity (which implies that the stress components are up to the third-order nonlinearity), and as a result we obtain

$$\begin{aligned}\Phi =&\frac{1}{2}(\xi_1\frac{U^2}{R^2} + \xi_3 U_Z^2 + 2\xi_2\frac{U}{R}W_Z + \xi_1 W_Z^2 + 2\xi_2\frac{U}{R}U_R + 2\xi_2 W_Z U_R + \xi_1 U_R^2 \\
&+ 2\xi_3 U_Z W_R + \xi_3 W_R^2) + \frac{1}{6}(\eta_1\frac{U^3}{R^3} + 3\eta_5\frac{U}{R}U_Z^2 + 3\eta_2\frac{U^2}{R^2}W_Z + 3\eta_4 U_Z^2 W_Z \\
&+ 3\eta_2\frac{U}{R}W_Z^2 + \eta_1 W_Z^3 + 3\eta_2\frac{U^2}{R^2}U_R + 3\eta_4 U_Z^2 U_R + 6\eta_3\frac{U}{R}W_Z U_R + 3\eta_2 W_Z^2 U_R \\
&+ 3\eta_2\frac{U}{R}U_R^2 + 3\eta_2 W_Z U_R^2 + \eta_1 U_R^3 + 6\eta_8\frac{U}{R}U_Z W_R + 6\eta_7 U_Z W_Z W_R \\
&+ 6\eta_7 U_Z U_R W_R + 3\eta_5\frac{U}{R}W_R^2 + 3\eta_4 W_Z W_R^2 + 3\eta_4 U_R W_R^2) \\
&+ \frac{1}{24}(\theta_1\frac{U^4}{R^4} + 6\theta_6\frac{U^2}{R^2}U_Z^2 + \theta_9 U_Z^4 + 4\theta_2\frac{U^3}{R^3}W_Z + 12\theta_8\frac{U}{R}U_Z^2 W_Z \\
&+ 6\theta_3\frac{U^2}{R^2}W_Z^2 + 6\theta_5 U_Z^2 W_Z^2 + 4\theta_2\frac{U}{R}W_Z^2 + \theta_1 W_Z^4 + 6\theta_3 W_Z^2 U_R^2 \\
&+ 12\theta_8\frac{U}{R}U_Z^2 U_R + 12\theta_4\frac{U^2}{R^2}W_Z U_R + 12\theta_7 U_Z^2 W_Z U_R + 4\theta_2\frac{U^3}{R^3}U_R \\
&+ 12\theta_4\frac{U}{R}W_Z^2 U_R + 4\theta_2 W_Z^3 U_R + 6\theta_3\frac{U^2}{R^2}U_R^2 + 6\theta_5 U_Z^2 U_R^2 + 12\theta_4\frac{U}{R}W_Z U_R^2 \\
&+ 4\theta_2\frac{U}{R}U_R^3 + 4\theta_2 W_Z U_R^3 + \theta_1 U_R^4 + 12\theta_{13}\frac{U^2}{R^2}U_Z W_R + 24\theta_{14} U_Z W_Z U_R W_R \\
&+ 24\theta_{15}\frac{U}{R}U_Z W_Z W_R + 12\theta_{12} U_Z W_Z^2 W_R^2 + 24\theta_{15}\frac{U}{R}U_Z U_R W_R + 4\theta_{16} U_Z^3 W_R \\
&+ 12\theta_{12} U_Z U_R^2 W_Z + 6\theta_6\frac{U^2}{R^2}W_R^2 + 6\theta_{17} U_Z^2 W_R^2 + 12\theta_8\frac{U}{R}W_Z W_R^2 + 6\theta_5 W_Z^2 W_R^2 \\
&+ 12\theta_8\frac{U}{R}U_R W_R^2 + 12\theta_7 W_Z U_R W_R^2 + 6\theta_5 U_R^2 W_R^2 + 4\theta_{16} U_Z W_R^3 + \theta_9 W_R^4).\end{aligned} \tag{5.1}$$

The strain energy per unit length is given by

$$\Psi = \int_0^a \int_0^{2\pi} \Phi R dR d\Theta. \tag{5.2}$$

By using the same manipulations in section 3 and section 4, we can get the average strain energy over a cross section

$$
\begin{aligned}
\widetilde{\Psi} =& \frac{\Psi}{\pi a^2} \\
=& \epsilon^2[(\xi_1+\xi_2)V_0^2 + 2\xi_2 V_0 W_{0z} + \frac{1}{2}\xi_1 W_{0z}^2 \\
&+ \epsilon((\frac{\eta_1}{3}+\eta_2)V_0^3 + (\eta_2+\eta_3)V_0^2 W_{0z} + \eta_2 V_0 W_{0z}^2 + \frac{\eta_1}{6}W_{0z}^3) \\
&+ \epsilon^2((\frac{\theta_1}{12}+\frac{\theta_2}{3}+\frac{\theta_3}{4})V_0^4 + (\frac{\theta_2}{3}+\theta_4)V_0^3 W_{0z} + (\frac{\theta_3}{2}+\frac{\theta_4}{2})V_0^2 W_{0z}^2 \\
&+ \frac{\theta_2}{3}V_0 W_{0z}^3 + \frac{\theta_1}{24}W_{0z}^4) + \nu(\frac{\xi_2^2}{4\xi_3}V_{0z}^2 + (\frac{\xi_2^2}{2\xi_1} - \frac{\xi_2^2}{4\xi_3} + \frac{\xi_2^3}{4\xi_1\xi_3})V_0 V_{0zz} \\
&+ (-\frac{\xi_1}{4} + \frac{\xi_2^2}{2\xi_1} - \frac{\xi_1\xi_2}{4\xi_3} + \frac{\xi_2^3}{4\xi_1\xi_3})W_{0z}V_{0zz} + \frac{\xi_1\xi_2}{4\xi_3}V_{0z}W_{0zz} + \frac{\xi_1^2}{16\xi_3}W_{0zz}^2 \\
&+ (\frac{\xi_1}{8} + \frac{\xi_2}{8} - \frac{\xi_1\xi_2}{8\xi_3} + \frac{\xi_2^2}{8\xi_3})V_0 W_{0zzz} + (\frac{\xi_2}{8} - \frac{\xi_1^2}{8\xi_3} + \frac{\xi_2^2}{8\xi_3})W_{0z}W_{0zzz}) \\
&+ \epsilon\nu(c_1 V_0 V_{0z}^2 + c_2 V_{0z}^2 W_{0z} + c_3 V_0^2 V_{0zz} + c_4 V_0 W_{0z} V_{0zz} + c_5 W_{0z}^2 V_{0zz} \\
&+ c_6 V_0 V_{0z} W_{0zz} + c_7 V_{0z} W_{0z} W_{0zz} + c_8 V_0 W_{0zz}^2 + c_9 W_{0z} W_{0zz}^2 + c_{10} V_0^2 W_{0zzz} \\
&+ c_{11} V_0 W_{0z} W_{0zzz} + c_{12} W_{0z}^2 W_{0zzz})],
\end{aligned}
\tag{5.3}
$$

where c_i $(i = 1, \cdots, 12)$ are some constants, whose expressions can be found in Appendix A.

By further using (4.12) and (4.13), we can reduce the above equation as

$$
\begin{aligned}
\widetilde{\Psi} =& \epsilon^2 E[\frac{1}{2}W_{0z}^2 - \frac{1}{8}\nu W_{0z}W_{0zzz} + \frac{1}{3}D_1\epsilon W_{0z}^3 \\
&+ \frac{1}{4}D_2\epsilon^2 W_{0z}^4 + \epsilon\nu(H_1 W_{0z}W_{0zz}^2 + H_2 W_{0z}^2 W_{0zzz})] \\
=& E[\frac{1}{2}V^2 + \frac{1}{3}D_1 V^3 + \frac{1}{4}D_2 V^4 - \frac{1}{8}a^2 V V_{ZZ} + a^2(H_1 V V_Z^2 + H_2 V^2 V_{ZZ})],
\end{aligned}
\tag{5.4}
$$

where

$$
H_1 = \frac{\xi_1^2(\eta_1+2\eta_2) + \xi_2^2(3\eta_1+2\eta_2-2\eta_3) + 2\xi_1\xi_2(\eta_1-2\eta_2-2\eta_3)}{8(\xi_1+\xi_2)(\xi_1^2+\xi_1\xi_2-2\xi_2^2)}, \tag{5.5}
$$

$$
\begin{aligned}
H_2 =&\frac{1}{16(\xi_1+\xi_2)^3(\xi_1^2+\xi_1\xi_2-2\xi_2^2)}[2\xi_1^5+\xi_1^4(8\xi_2-\eta_2)\\
&+\xi_2^4(3\eta_1+14(\eta_2-\eta_3))+2\xi_1^3\xi_2(3\xi_2-\eta_1+\eta_3)\\
&+\xi_1^2\xi_2^2(-8\xi_2-7\eta_1+11\eta_2+2\eta_3)-2\xi_1\xi_2^3(4\xi_2+3\eta_1-6\eta_2+7\eta_3)].
\end{aligned} \tag{5.6}
$$

The total potential energy is then given by

$$
\begin{aligned}
\Omega =& \int_{-l}^{l}\Psi dZ - T\int_{-l}^{l} V dZ = \pi a^2 (\int_{-l}^{l}\widetilde{\Psi} dZ - E\int_{-l}^{l}\gamma V dZ)\\
=&\pi a^2 E\int_{-l}^{l}(-\gamma V+\frac{1}{2}V^2+\frac{1}{3}D_1V^3+\frac{1}{4}D_2V^4-\frac{1}{8}a^2VV_{ZZ}\\
&+a^2(H_1VV_Z^2+H_2V^2V_{ZZ}))dZ.
\end{aligned} \tag{5.7}
$$

Further by the variational principle, from the Euler-lagrange equation we obtain

$$
V+D_1V^2+D_2V^3+a^2[-\frac{1}{4}V_{ZZ}+(2H_2-H_1)V_Z^2+2(2H_2-H_1)VV_{ZZ}]=\gamma. \tag{5.8}
$$

It can be seen from (5.5), (5.6) and (4.21) that $2H_2-H_1=D_3$. So the equation (5.8) is exactly the equation (4.25).

The expressions of $\tilde{\Psi}$ and Ω are themselves important. When there are multiple solutions, the smallest energy criterion can be used to judge the preferred solution (configuration).

6 The clamped boundary conditions

Now, we conduct a detailed analysis on the normal form equation with clamped end boundary conditions. We suppose that the strain energy function is non-convex in a homogeneous constant strain state such that phase transition can take place. This requires

$$
D_1<0, \quad D_2>0, \quad 3D_2<D_1^2<4D_2. \tag{6.1}
$$

We rewrite equation (4.25) as a first-order system

$$\begin{aligned} V_Z &= y \\ y_Z &= \frac{V + D_1 V^2 + D_2 V^3 + D_3 a^2 y^2 - \gamma}{a^2(\frac{1}{4} - 2D_3 V)}. \end{aligned} \tag{6.2}$$

The critical points of this system are determined by $y = 0$ and

$$V + D_1 V^2 + D_2 V^3 = \gamma. \tag{6.3}$$

In this paper, we always choose $D_1 = -18$, $D_2 = 100$. We can see that with these material constants, the critical stress values γ_1, γ_2, γ_m (cf. (6.4)) and the corresponding strain values (cf. Figure 1) are close to the experimental results (Tse & Sun 2000 and Li & Sun 2002). The $\gamma - V$ curve corresponding to equation (6.3) is shown in Figure 1.

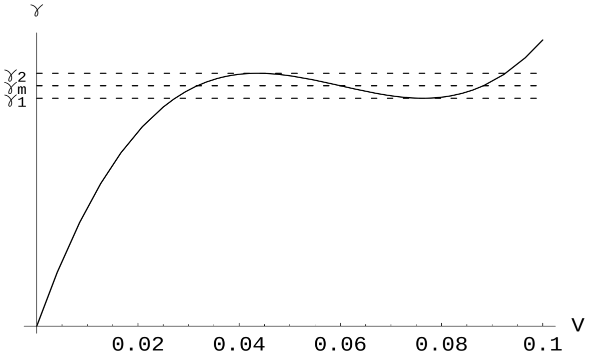

Figure 1. The $\gamma - V$ curve corresponding to (6.3).

The peak stress value γ_2, the valley stress value γ_1 and the Maxwell stress value γ_m are

$$\begin{aligned} \gamma_1 =& \frac{2D_1^3 - 2(D_1^2 - 3D_2)^{\frac{3}{2}} - 9D_1D_2}{27D_2^2} = 0.015929070313677, \\ \gamma_2 =& \frac{2D_1^3 + 2(D_1^2 - 3D_2)^{\frac{3}{2}} - 9D_1D_2}{27D_2^2} = 0.017670929686323, \\ \gamma_m =& \frac{2D_1^3 - 9D_1D_2}{27D_2^2} = 0.016800000000000. \end{aligned} \tag{6.4}$$

The natural boundary conditions $V_Z = 0$ at the two ends have been used by many authors (e.g., Ericksen 1975; Tong *et al.* 2001; Cai & Dai 2006). However, such conditions are difficult to be realized in practice. In experiments, usually the two ends are clamped into the rigid bodies. To better describe the realistic situation, in this paper we will consider the case that the two ends of the cylinder are clamped into rigid constraints. In this case, we can propose the conditions according to the fact that there is no radial displacement for the point at the lateral surface of the ends, i.e.,

$$U|_{R=a} = 0, at \;\; Z = -l, l. \tag{6.5}$$

By using (3.1), (3.2) and (4.2), neglecting the $O(\nu^2)$ terms, we obtain

$$V_0 + \nu V_1 = 0, at \; z = -l, l. \tag{6.6}$$

In deriving equation (4.18), V_0 and V_1 have been expressed in terms of W_0. Using such relations in equation (6.6) and with the help of equation (4.25), we obtain

$$F_1 V + F_2 V^2 + F_3 V^3 = \gamma, \quad at \;\; Z = -l, l. \tag{6.7}$$

where F_1, F_2 and F_3 are material constants. Notice that in deriving (6.7) we have neglected the terms higher than $O(\epsilon^2, \nu)$. It's clear that if we choose different values of F_1, F_2 and F_3, the properties of the boundary condition (6.7) may also have a lot of differences. Here we will only consider a simple case. We will choose F_1, F_2 and F_3 such that the cubic equation (6.7) has only one unique positive root V_e when $\gamma > 0$, and this root is much smaller than the positive roots of equation (6.3). In this paper, we will choose $F_1 = 3$, $F_2 = -20$ and $F_3 = 100$ to get the following graphic result:

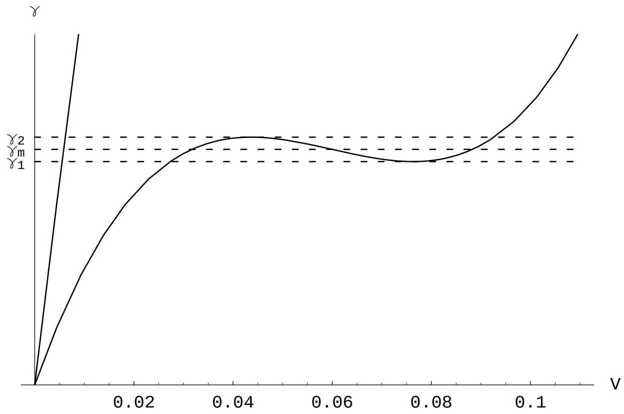

Figure 2. Relationship between the $\gamma - V$ curves corresponding to (6.3) and (6.7).

Thus the boundary conditions at the two ends are

$$V = V_e \quad at \;\; Z = -l, l. \tag{6.8}$$

We note that V_e depends on the value of the engineering stress γ.

Remark: Although the normal form equation is one-dimensional, it is derived from a three-dimensional setting, and as a result we can use the end conditions by considering the quantities in the radial dimension. If one directly introduces a one-dimensional model, such an option is not available.

7 Asymptotic solutions

We now consider the solutions for a given engineering stress γ under the clamped boundary conditions (6.8). In the following, without loss of generality, we take $l = 1$. Then in equation (4.25), a is equivalent to the diameter-length ratio. Due to symmetry, we only consider the part $0 \le Z \le 1$ and boundary conditions (6.8) can be replaced by

$$V_Z|_{Z=0} = 0, \qquad V|_{Z=1} = V_e. \tag{7.1}$$

7.1 Force-controlled problem

We regard the engineering stress γ as the bifurcation parameter. As γ varies, there are seven types of phase planes, which are shown in Figure 3.

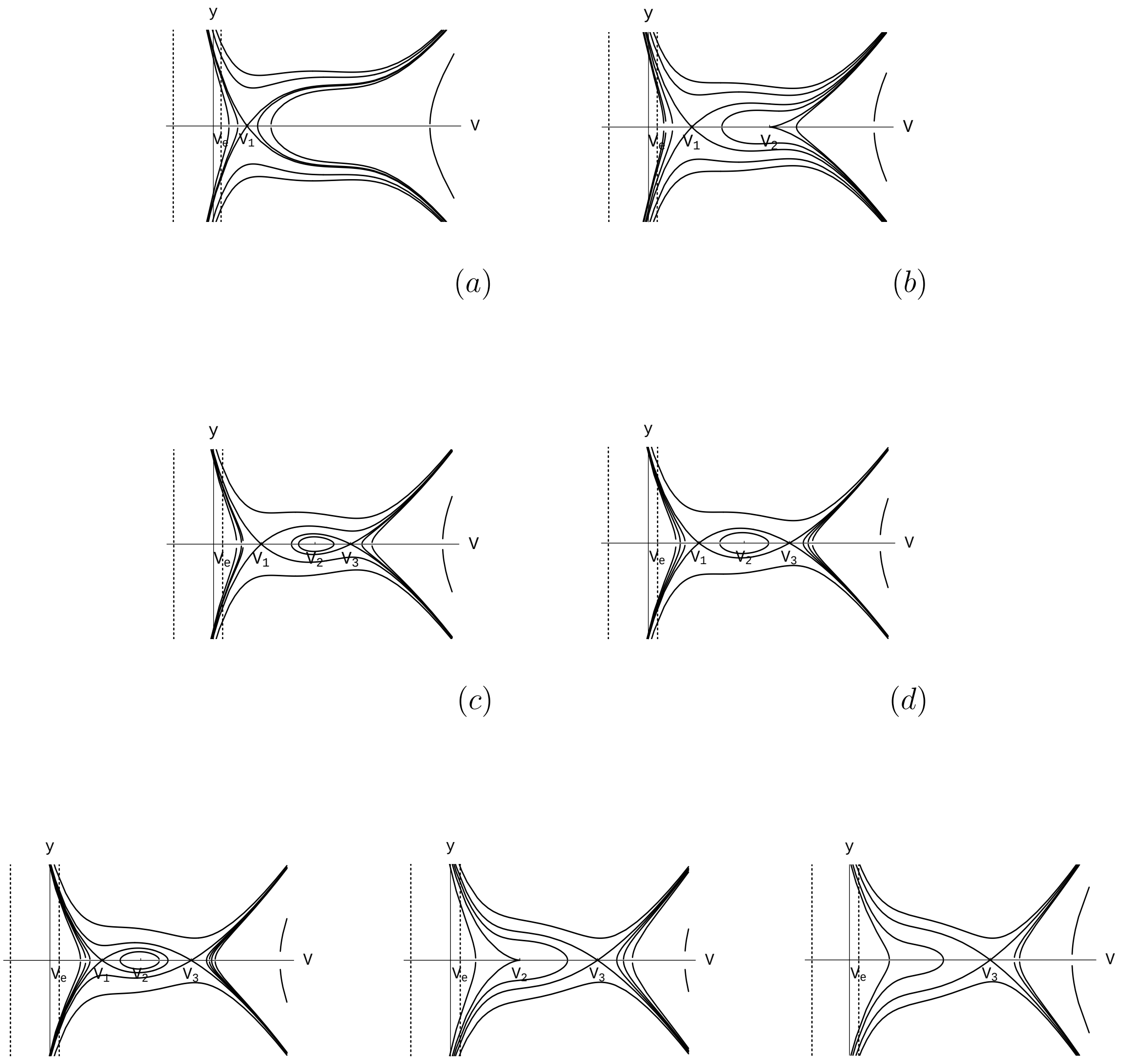

(a) (b) (c) (d) (e) (f) (g)

Figure 3. Phase planes as the external stress γ varies. (a) $0 \leq \gamma \leq \gamma_1$, (b) $\gamma = \gamma_1$, (c) $\gamma_1 < \gamma < \gamma_m$, (d) $\gamma = \gamma_m$, (e) $\gamma_m < \gamma < \gamma_2$, (f) $\gamma = \gamma_2$, (g) $\gamma > \gamma_2$.

Every trajectory in the phase planes of Figure 3 is a solution of the system (6.2). However, only those trajectories that satisfy equation (7.1) represent the physical solutions for the present problem. It can be seen that for a trajectory to be the physical solution a necessary and sufficient condition is that it contacts the V-axis once (so that $V_Z|_{Z=0} = 0$) and contacts the vertical line $V = V_e$ once (so that $V|_{Z=1} = V_e$) and the Z-interval for this segment of the trajectory is exactly equal to 1.

To deduce the solution, we integrate (4.25) once to obtain

$$H - \gamma V + \frac{1}{2}V^2 + \frac{1}{3}D_1V^3 + \frac{1}{4}D_2V^4 + a^2(-\frac{1}{8}V_Z^2 + D_3VV_Z^2) = 0, \tag{7.2}$$

where H is the integration constant. If one trajectory contact the V-axis at point $(v_0, 0)$, v_0 must be a real root of the equation

$$H - \gamma V + \frac{1}{2}V^2 + \frac{1}{3}D_1V^3 + \frac{1}{4}D_2V^4 = 0 \tag{7.3}$$

By using (7.2) and consider the case $0 \leq Z \leq 1$, we can get

$$\begin{aligned} \frac{dV}{dZ} &= -\sqrt{\frac{H - \gamma V + \frac{1}{2}V^2 + \frac{1}{3}D_1V^3 + \frac{1}{4}D_2V^4}{a^2(\frac{1}{8} - D_3V)}} \\ &= -\sqrt{\frac{-D_2}{4a^2D_3}}\sqrt{\frac{\frac{4H}{D_2} - \frac{4\gamma}{D_2}V + \frac{2}{D_2}V^2 + \frac{4D_1}{3D_2}V^3 + V^4}{V - \beta}}, \end{aligned} \tag{7.4}$$

with $\beta = \frac{1}{8D_3}$. Here, for simplicity, we choose $D_3 = -5$ such that $\beta < 0$ for graphic results. Suppose that $V|_{Z=0} = v_0$, we can obtain

$$Z = -2a\sqrt{\frac{D_3}{-D_2}}\int_{v_0}^{V}\sqrt{\frac{\tau - \beta}{\frac{4H_0}{D_2} - \frac{4\gamma}{D_2}\tau + \frac{2}{D_2}\tau^2 + \frac{4D_1}{3D_2}\tau^3 + \tau^4}}d\tau, \quad V_e \leq V \leq v_0, \tag{7.5}$$

where

$$H_0 = -(-\gamma v_0 + \frac{1}{2}v_0^2 + \frac{1}{3}D_1v_0^3 + \frac{1}{4}D_2v_0^4).$$

To satisfy the end boundary condition (7.1), we need to choose v_0 such that

$$-2a\sqrt{\frac{D_3}{-D_2}}\int_{v_0}^{V_e}\sqrt{\frac{\tau-\beta}{\frac{4H_0}{D_2}-\frac{4\gamma}{D_2}\tau+\frac{2}{D_2}\tau^2+\frac{4D_1}{3D_2}\tau^3+\tau^4}}d\tau = 1. \tag{7.6}$$

Based on the phase planes in Figure 3 and equation (7.5) and (7.6), we can construct all the possible solutions for a given γ.

Case (a) $0 < \gamma \le \gamma_m$ (cf. Figure 3(a)-3(d))

In this case, from Figure 3(a)-3(d), we can see that only the trajectories located between the left saddle point V_1 and the vertical line $V = V_e$ (notice that $V_e \ll V_1$, cf. Figure 2) can be the possible solutions.

For any given γ, V_e and V_1 can be calculated immediately from the two equations (6.3) and (6.7). By using the equation (7.6), we can determine the value of v_0. Once v_0 is determined, through numerical integration, the corresponding solution can be obtained from (7.5).

For any γ satisfies $0 < \gamma \le \gamma_m$, we found that there is only one solution (denoted by S_1), which is very close to the saddle point V_1.

Case (b) $\gamma_m < \gamma < \gamma_2$ (cf. Figure 3(e))

In this case, for some given γ, there are multiple solutions.

From figure 3(e), we can see that the trajectories located between the left saddle point V_1 and the vertical line $V = V_e$ can be the possible solutions. Through some calculations, we found that for any $\gamma_m < \gamma < \gamma_2$, there exist one solution (also denoted by S_1), which is represented by a trajectory to the left of (also very close to) the saddle point V_1.

We can see that the trajectories located between the homoclinic orbit and the right saddle point V_3 can also be the possible solutions. Through some calculations, we found that there is a critical engineering stress $\gamma_p = \gamma_p(a)$ which satisfies $\gamma_m < \gamma_p(a) < \gamma_2$. When $\gamma_p(a) < \gamma < \gamma_2$, there exist another two solutions. One solution (denoted by S_2) is represented by a trajectory outside (but very close) to the homoclinic orbit. The other solution (denoted by S_3) is represented by a trajectory outside the second one and to the left of (very close to) the right saddle point V_3.

Thus the critical engineering stress $\gamma_p(a)$ can be considered as a bifurcation point. When $\gamma_m < \gamma < \gamma_p(a)$, there is only one solution. When $\gamma_p(a) < \gamma < \gamma_2$, there are three solutions. We found that $\gamma_p(a)$ is a monotonically increasing function of the diameter-length ratio a, e.g., $\gamma_p(0.03) = 0.0168005239556$, $\gamma_p(0.06) = 0.0168907218423$.

Case (c) $\gamma = \gamma_2$ (cf. Figure 3(f))

In this case, there are three solutions. The first solution (also denoted by S_1) is represented by a trajectory to the left of (also very close to) the cusp point V_2. The second solution (also denoted by S_2) is represented by a trajectory to the right of (also very close to) the cusp point V_2. The third solution (also denoted by S_3) is represented by a trajectory to the left of (also very close to) the saddle point V_3.

Case (d) $\gamma > \gamma_2$ (cf. Figure 3(g))

In this case, there exist another critical engineering stress $\gamma_q = \gamma_q(a)$ which is a little bit larger than γ_2.

When $\gamma_2 < \gamma < \gamma_q(a)$, there are three solutions. The first two solutions (also denoted by S_1 and S_2) are represented by two trajectories (very close to each other) located in the middle part of the interval (V_e, V_3). The third solution (also denoted by S_3) is represented by a trajectory to the left of (very close to) the saddle point V_3. When $\gamma > \gamma_q(a)$, there is only one solution (also denoted by S_3), which is represented by a trajectory to the left of (very close to) the saddle point V_3.

Thus the critical engineering stress $\gamma_q(a)$ can be considered as another bifurcation point. We found that $\gamma_q(a)$ is also a monotonically increasing function of the diameter-length ratio a, e.g., $\gamma_q(0.03) = 0.017677609814$, $\gamma_q(0.06) = 0.017735345200$.

For the radius $a = 0.03$, the axial strain distribution $V(Z)$ corresponding to the above four cases are plotted in Figure 4.

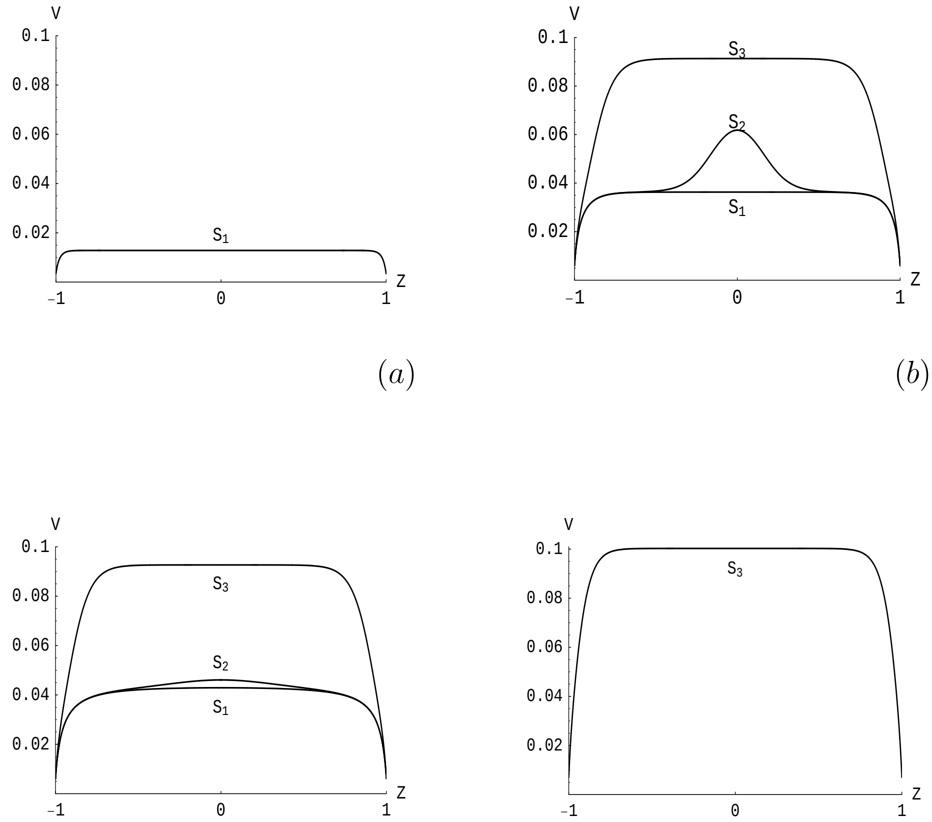

(a) (b)

(c) (d)

Figure 4. The axial strain distribution curves for four different γ values ($a = 0.03$): (a) $0 < \gamma = 0.010080 < \gamma_p$, (b) $\gamma_p < \gamma = 0.017366 < \gamma_2$, (c)$\gamma = \gamma_2$, (d) $\gamma = 0.020114 > \gamma_q$.

From the above results, it can be seen that there are multiple solutions for $\gamma_p(a) < \gamma < \gamma_q(a)$. We suppose that the preferred solution should be the one which has the smallest total potential energy value. To determine which solution is the most preferred one, we consider the total potential energy values of all the possible solutions. From (5.7) and due to symmetric, we can get

$$\Omega = 2\pi a^2 E \int_0^1 (-\gamma V + \frac{1}{2}V^2 + \frac{1}{3}D_1 V^3 + \frac{1}{4}D_2 V^4 - \frac{1}{8}a^2 V V_{ZZ} + a^2(H_1 V V_Z^2 + H_2 V^2 V_{ZZ}))dZ, \tag{7.7}$$

Without loss of generality, we choose $H_1 = 15$ and $H_2 = 5$ for graphic results. For the radius $a = 0.03$, we plot the total potential energies for all the solutions in Figure 5.

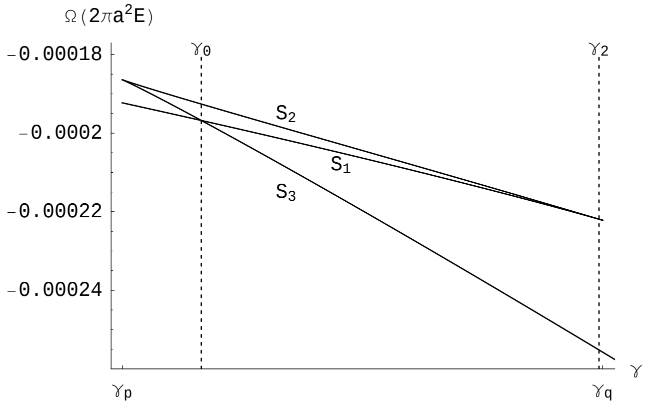

Figure 5. Relationships between γ and the potential energies ($a = 0.03$).

From figure 5, it can be seen that there is a critical stress value $\gamma_0 = \gamma_0(a)$ (e.g., $\gamma_0(0.03) = 0.01694471757$). For $\gamma_p < \gamma < \gamma_0$, the first solution S_1 is the preferred solution, and for $\gamma_0 < \gamma < \gamma_q$, the third solution S_3 is the preferred solution. Thus, in a loading process, after $\gamma > \gamma_0$, the configuration of the cylinder may jump from solution S_1 towards solution S_3, which is corresponding to the phase transition process.

Remark: The existence of $\gamma_0(a)$ $(> \gamma_p(a) > \gamma_m)$ is significant and it implies that under clamped end conditions the phase transition can only happen at a stress value larger than the Maxwell stress.

7.2 Displacement-controlled problem

We now consider the case that the total elongation

$$\int_{-l}^{l} V dZ = 2 \int_{0}^{l} V dZ = 2\Delta \tag{7.8}$$

is given. Since we have taken l to be 1, Δ is actually the engineering strain. The governing equation is still equation (4.25), but now γ is an unknown parameter.

In the previous section, we have obtained all the solutions for a given γ. If for a given Δ we can find the corresponding value γ, then we can obtain the solutions for a displacement-controlled problem.

We first plot the $\gamma - \Delta$ curves corresponding to the solutions we obtained in the previous section for four different values of a in Figure 6.

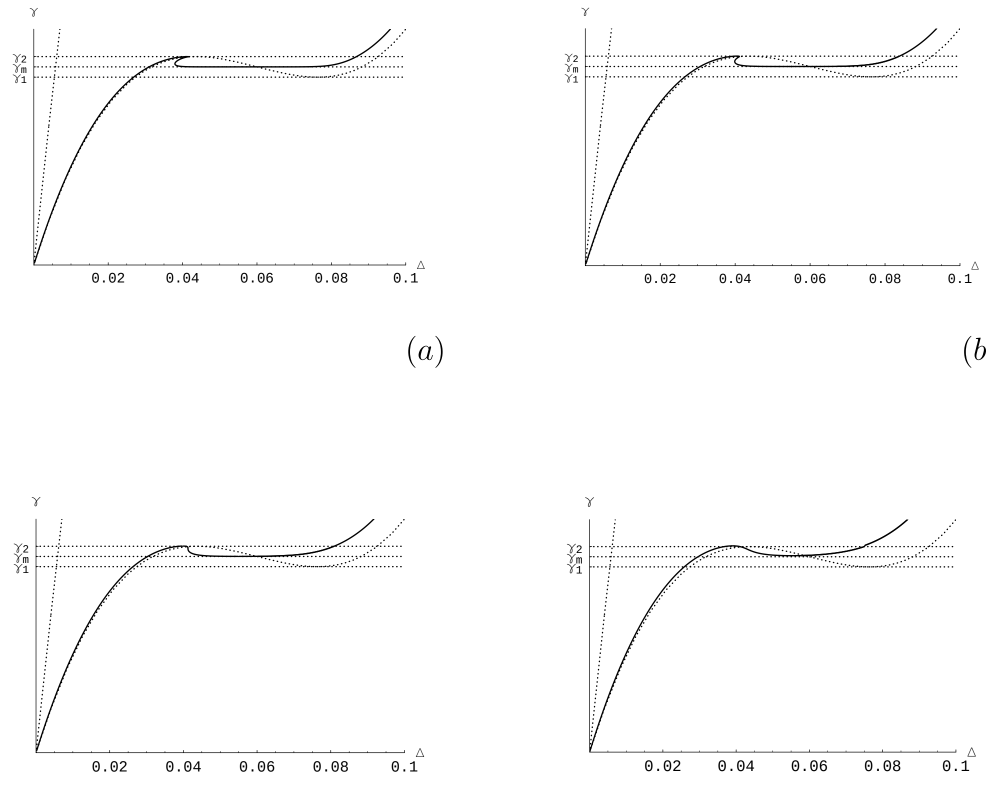

(a) (b)

(c) (d)

Figure 6. The engineering $\gamma - \Delta$ curves for different values of a: (a) $a = 0.02$; (b) $a = 0.03$; (c) $a = 0.04$; (d) $a = 0.06$. The dashed lines are the curves shown in Figure 2.

We can see that the $\gamma - \Delta$ curves shown in Figure 6 have some important features.

First, these curves obtained from the asymptotic solutions capture the main characteristics of the engineering stress-strain curves measured in a number of experiments (Shaw & Kyriakides 1995, Sun *et al.* 2000, Tse & Sun 2000, Favier *et al.* 2001 and Li & Sun 2002), i.e., there is a stress peak, which is followed by a sharp stress drop, and then there is a stress plateau (cf. Figure 6(c)).

Second, it can be seen that there is a snap-back when the diameter-length ratio a is small (cf. Figure 6(a) and 6(b)). As the diameter-length ratio become larger, this snap-back phenomenon disappear (cf. Figure 6(c) and 6(d)).

Third, as the diameter-length ratio a increases, the whole $\gamma - \Delta$ curve moves towards left, especially in the high-strain region. It is clear that this feature is due to the boundary effect.

With these curves, we are ready to convert the solutions of a force-controlled problem into those of a displacement-controlled problem. As we pointed out that if the diameter-length ratio a is large enough, there is no snap-back on the corresponding $\gamma - \Delta$ curve (cf. Figure 6(c) and 6(d)). Thus, in this case, for a given displacement Δ, we can only get one corresponding stress value γ from the $\gamma - \Delta$ curve. For this γ, there is a unique phase plane. There are maybe more than one trajectories in this phase plane which satisfy the end boundary conditions, however only one of them can give the required displacement value, which then represents the unique solution for the given Δ.

As we pointed out before that the normal form equation (4.25) is derived from the three-dimensional field equations. With the solutions of the normal form equation, we can recover the three-dimensional strain fields. Here, we take $a = 0.04$ as an example. Corresponding to the four points $A - D$ shown in Figure 7,

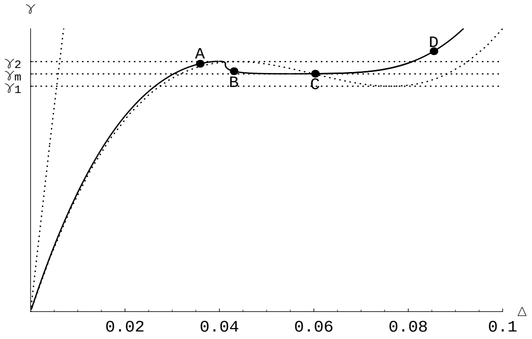

Figure 7. The engineering $\gamma - \Delta$ curve for $a = 0.04$.

we draw the shapes of the cylinder in Figure 8 (the radial deformation has been enlarged for clearness).

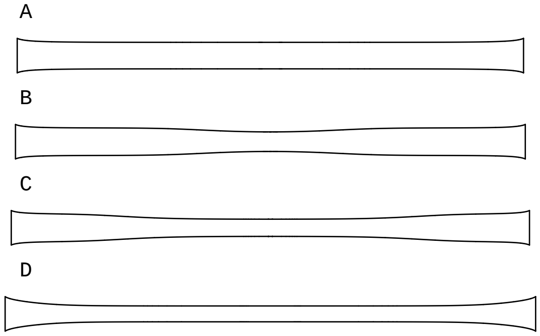

Figure 8. Cylinder shapes in different total elongations for the case $a = 0.04$: (a) $\Delta = 0.035882224$; (b) $\Delta = 0.043065200$; (c) $\Delta = 0.060283469$; (d) $\Delta = 0.085396683$.

Figure 8(a) represents a low-strain state, Figure 8(b) represents a transition state, Figure 8(c) represents a two-phase state, and Figure 8(d) represents a high-strain state. As the end displacement increases these four states appears consecutively. Here, the asymptotic solutions we obtained can describe the whole deformation process. We know that the dimensionless engineering stress γ represent the stress density acting on the cross section of the cylinder in the reference configuration. Now, based on the solutions obtained, we can also calculate the true stress density σ acting on the cross section of the cylinder in the current configuration. Figure 9 shows the distributions of the true stress σ corresponding to the four points $A - D$. We see, very interesting, the true stress actually decreases from A to B and to C. We also point out that a pure one-dimensional model cannot yield the true stress distribution.

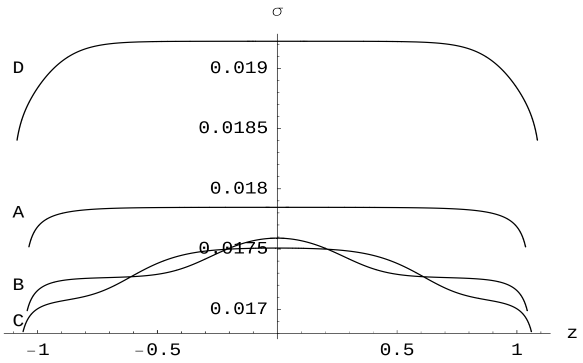

Figure 9. The distributions of the true stress density σ acting on the cross section of the cylinder in the current configuration.

If the diameter-length ratio a is relatively small, we know that there is a snap-back on the corresponding $\gamma - \Delta$ curve (cf. Figure 6(a) and 6(b)). Thus, for the total elongation Δ located in some special region, there may exist multiple corresponding stress values γ, i.e., the solutions are not unique. Then we need to determine which solution is the preferred one.

We take $a = 0.02$ as an example. From Figure 10, we can see that when $\Delta_1 < \Delta < \Delta_2$, there are three possible solutions, which are labeled as U_1, U_2 and U_3, respectively.

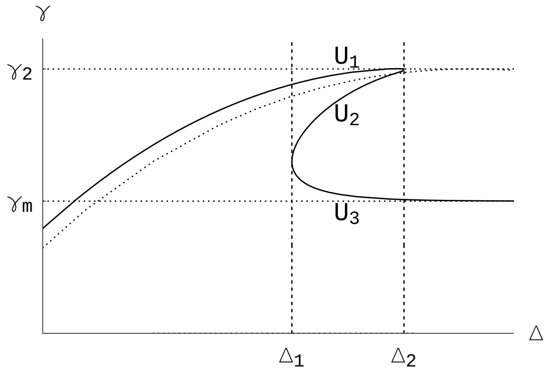

Figure 10. Snap-back on the $\gamma - \Delta$ curve for $a = 0.02$.

To choose the preferred solution from U_1, U_2 and U_3, we calculate the total potential energy values of these solutions. Denote Ω^* the total potential energy of the cylinder in the displacement-controlled problem and we have

$$\begin{aligned}\Omega^* = 2\pi a^2 E \int_0^1 \Big(\frac{1}{2}V^2 + \frac{1}{3}D_1 V^3 + \frac{1}{4}D_2 V^4 - \frac{1}{8}a^2 V V_{ZZ} \\ + a^2(H_1 V V_Z^2 + H_2 V^2 V_{ZZ})\Big) dZ.\end{aligned} \tag{7.9}$$

Here we still choose $H_1 = 15$, $H_2 = 5$. In Figure 11, we plot the differences of the total potential energies between solutions U_2, U_3 and solution U_1 for $\Delta_1 < \Delta < \Delta_2$.

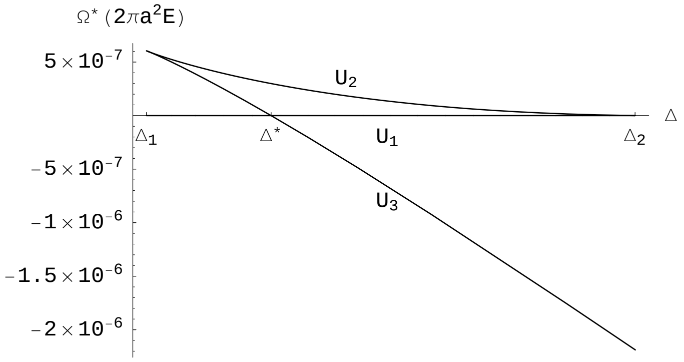

Figure 11. Differences of the total potential energies between solutions U_2, U_3 and solution U_1 for $\Delta_1 < \Delta < \Delta_2$ ($a = 0.02$).

From Figure 11, we can see that for $\Delta_1 < \Delta < \Delta^*(= 0.038848990)$, solution U_1 is the preferred solution and for $\Delta^* < \Delta < \Delta_2$, solution U_3 is the preferred solution. The engineering stress-strain curve corresponding to the preferred solution is shown in Figure 12.

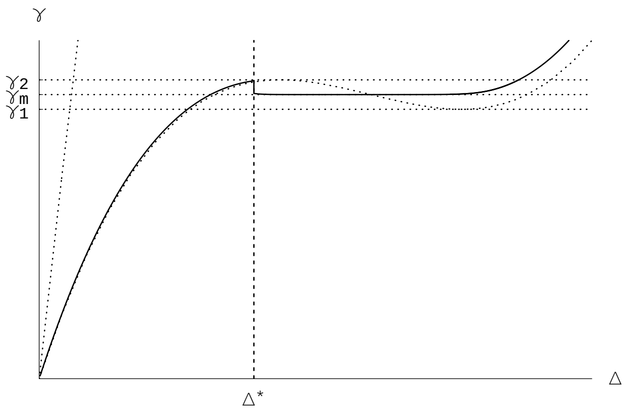

Figure 12. The engineering stress-strain curve corresponding to the preferred solution for $a = 0.02$.

It is worth to note that there exists a jump for the stress γ at $\Delta = \Delta^*$. This curve also captures the main features of the experimental results in the loading process (Shaw & Kyriakides 1995, Sun *et al.* 2000, Tse & Sun 2000, Favier *et al.* 2001 and Li & Sun 2002).

Figure 13 shows the true stress-strain (σ-Δ) curves (occurring at $Z = 0$ and $Z = 0.6$) corresponding to the preferred solutions for $a = 0.02$.

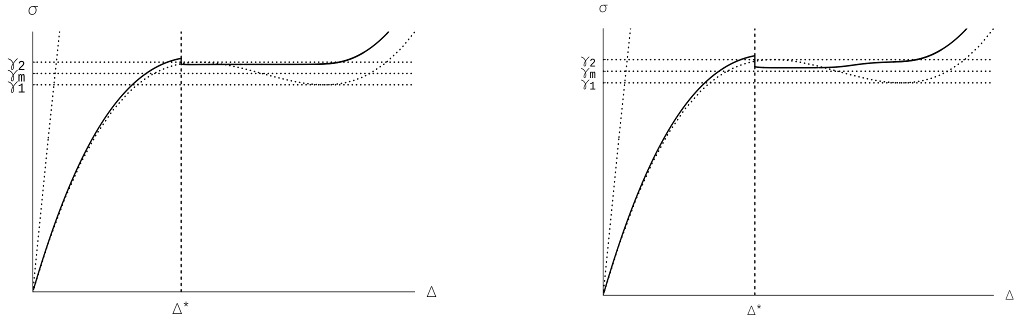

(*a*) (*b*)

Figure 13. The true stress-strain curves. (a) occurring at $Z = 0$ for $a = 0.02$; (b) occurring at $Z = 0.6$ for $a = 0.02$.

It is worth to note that for the case occurring at $Z = 0$, the drop for σ become very small and after that there is also a stress plateau (with the true stress value larger than the Maxwell stress). For the case occurring at $Z = 0.6$, the drops for σ become larger. But now the stress plateaus have been divided into two parts, which corresponding to the fact that phase transition first start at the middle part of the cylinder and transform gradually towards the two ends.

8 Conclusions

We consider phase transitions induced by axial tension/extension in a slender circular cylinder composed of a general compressible hyperelastic material with a non-convex strain energy function under clamped end conditions. In order to capture the macroscopic phenomena observed in the experiments by others, the problem is formulated in a three-dimensional setting and as a result it is governed by a system of coupled nonlinear PDE's with complicated nonlinear boundary conditions. A novel approach involving coupled series-asymptotic expansions is developed to derive the normal form equation (NFE) of the original system. By conducting the phase-plane analysis on this NFE, we manage to deduce the global bifurcation properties of its solutions. The solutions (including those for post-bifurcation solutions) for both a force-controlled problem and a displacement-controlled problem are obtained. These asymptotic solutions demonstrate the essential features of phase transitions in a cylinder and are consistent with the experimental data qualitatively. Specifically, the engineering stress-strain curve is shown to have the same features as observed in experiments. These qualitative agreements with experiments give strong supporting evidence that a non-convex strain energy function can be used to describe phase transitions and the non-convexity of the strain energy function is the main cause of the instability phenomena associated with phase transitions in a slender cylinder. An important finding is that under the clamped end conditions, there exists a critical stress value $\gamma_0(a)$, which depends on the radius-length ratio and larger than the Maxwell stress, such that phase transition can only happen when the engineering stress is larger than this value. This is different from the case of the nature boundary condition that phase transition can happen as long as the engineering stress is larger than the Maxwell stress.

Acknowledgments

The work described in this paper was fully supported by two grants from the Research Grants Council of the HKSAR, China (Project numbers: CityU 100804 and CityU 100807).

Appendix A Incremental elastic moduli

For initially isotropic material, in the case that there are no prestresses, Φ should be a function of the principle stretches λ_1, λ_2 and λ_3, namely $\Phi{=}\Phi(\lambda_1, \lambda_2, \lambda_3)$. Denote by $\Phi_j = \frac{\partial \Phi}{\partial \lambda_j}|_{\lambda_1=\lambda_2=\lambda_3=1}$, then $\Phi_1 = \Phi_2 = \Phi_3$ should vanish since there are no prestresses.

The non-zero first order incremental elastic moduli can be written as

$$\begin{aligned}
\xi_1 &= a^1_{1111} = \Phi_{11}, \\
\xi_2 &= a^1_{1122} = \Phi_{12}, \\
\xi_3 &= a^1_{1212} = \frac{1}{2}(\xi_1 - \xi_2), \\
\xi_4 &= a^1_{1221} = \xi_3.
\end{aligned}$$

There are only two independent constants among ξ_i.

The non-zero second order incremental elastic moduli can be written as

$$
\begin{aligned}
\eta_1 &= a^2_{111111} = \Phi_{111},\\
\eta_2 &= a^2_{111122} = \Phi_{112},\\
\eta_3 &= a^2_{112233} = \Phi_{123},\\
\eta_4 &= a^2_{111212} = \frac{1}{4}(2\xi_2 + 2\xi_3 + \eta_1 - \eta_2),\\
\eta_5 &= a^2_{331212} = \frac{1}{2}(\xi_2 + \eta_2 - \eta_3),\\
\eta_6 &= a^2_{121323} = \frac{1}{2}(\eta_4 - \eta_5),\\
\eta_7 &= a^2_{111221} = \eta_4 - \xi_2 - \xi_3,\\
\eta_8 &= a^2_{331221} = \eta_5 - \xi_2,\\
\eta_9 &= a^2_{123123} = \eta_6 - \xi_3.
\end{aligned}
$$

There are only three additional independent constants among η_i.

The non-zero third order incremental elastic moduli can be written as

$$
\begin{aligned}
\theta_1 &= a^3_{11111111} = \Phi_{1111},\\
\theta_2 &= a^3_{11111122} = \Phi_{1112},\\
\theta_3 &= a^3_{11112222} = \Phi_{1122},\\
\theta_4 &= a^3_{11112233} = \Phi_{1123},\\
\theta_5 &= a^3_{11111212} = -\frac{1}{12}(6\xi_2 + 6\xi_3 - 3\eta_1 - 3\eta_2 - 2\theta_1 + 2\theta_2),\\
\theta_6 &= a^3_{11112323} = \frac{1}{2}(\eta_2 + \theta_3 - \theta_4),\\
\theta_7 &= a^3_{11221212} = -\frac{1}{2}(6\xi_2 + 6\xi_3 - 6\eta_2 - \theta_1 - 2\theta_2 + 3\theta_3),\\
\theta_8 &= a^3_{11221313} = -\frac{1}{4}(\xi_2 - \eta_2 - \eta_3 - \theta_2 + \theta_4),\\
\theta_9 &= a^3_{12121212} = \frac{1}{8}(6\xi_2 + 6\xi_3 + 6\eta_1 - 6\eta_2 + \theta_1 - 4\theta_2 + 3\theta_3),
\end{aligned}
$$

$$\begin{aligned}
\theta_{10} &= a^3_{12121313} = \frac{1}{3}\theta_9, \\
\theta_{11} &= a^3_{11121323} = -\frac{1}{24}(3\xi_1 - 3\eta_2 + 3\eta_3 - \theta_1 + \theta_2 + 3\theta_3 - 3\theta_4), \\
\theta_{12} &= a^3_{11111221} = \frac{1}{12}(6\xi_2 + 6\xi_3 - 3\eta_1 - 3\eta_2 + 2\theta_1 - 2\theta_2), \\
\theta_{13} &= a^3_{11112332} = -\frac{1}{2}(\eta_2 - \theta_3 + \theta_4), \\
\theta_{14} &= a^3_{11221221} = \frac{1}{12}(6\xi_2 + 6\xi_3 - 6\eta_2 + \theta_1 + 2\theta_2 - 3\theta_3), \\
\theta_{15} &= a^3_{11221331} = \frac{1}{4}(\xi_2 - \eta_2 - \eta_3 + \theta_2 - \theta_4), \\
\theta_{16} &= a^3_{12121221} = -\frac{1}{8}(6\xi_2 + 6\xi_3 - \theta_1 + 4\theta_2 - 3\theta_3), \\
\theta_{17} &= a^3_{12211221} = \frac{1}{8}(6\xi_2 + 6\xi_3 - 2\eta_1 + 2\eta_2 + \theta_1 - 4\theta_2 + 3\theta_3), \\
\theta_{18} &= a^3_{12121331} = \frac{1}{3}\theta_{16}, \\
\theta_{19} &= a^3_{12211331} = \frac{1}{24}(6\xi_1 - 3\eta_1 - 3\eta_2 + 6\eta_3 + \theta_1 - 4\theta_2 + 3\theta_3), \\
\theta_{20} &= a^3_{11123123} = \frac{1}{24}(6\xi_1 + 3\xi_2 - 3\eta_1 + 3\eta_3 + \theta_1 - \theta_2 - 3\theta_3 + 3\theta_4), \\
\theta_{21} &= a^3_{11123132} = \theta_{20} - \frac{1}{4}(\xi_1 + \xi_2 - \eta_1 + \eta_2), \\
\theta_{22} &= a^3_{12122323} = \frac{1}{24}(6\xi_2 - 6\xi_3 + 12\eta_2 - 12\eta_3 + \theta_1 - 4\theta_2 + 3\theta_3).
\end{aligned}$$

There are only four additional independent constants among θ_i.

The expressions of the constants c_i $(i = 1, \cdots, 12)$ in equation (5.3) are given below:

$$\begin{aligned}
c_1 =& \frac{\eta_2}{4} + \frac{\xi_2\eta_2}{4\xi_1} + \frac{\xi_2\eta_2}{4\xi_3} + \frac{\xi_2^2\eta_2}{4\xi_1\xi_3} + \frac{\eta_3}{4} + \frac{\xi_2\eta_3}{4\xi_1} + \frac{\xi_2\eta_3}{4\xi_3} + \frac{\xi_2^2\eta_3}{4\xi_1\xi_3} - \frac{3\eta_4}{4} - \frac{5\xi_2\eta_4}{4\xi_1} \\
&- \frac{3\xi_2^2\eta_4}{8\xi_3^2} - \frac{5\xi_2^3\eta_4}{8\xi_1\xi_3^2} - \frac{3\xi_2\eta_4}{4\xi_3} - \frac{5\xi_2^2\eta_4}{4\xi_1\xi_3} + \frac{\eta_5}{4} - \frac{\xi_2\eta_5}{4\xi_1} + \frac{\xi_2^2\eta_5}{8\xi_3^2} - \frac{\xi_2^3\eta_5}{8\xi_1\xi_3^2} + \frac{\xi_2\eta_5}{4\xi_3} \\
&- \frac{\xi_2^2\eta_5}{4\xi_1\xi_3} + \frac{3\eta_7}{4} + \frac{5\xi_2\eta_7}{4\xi_1} + \frac{3\xi_2\eta_7}{4\xi_3} + \frac{5\xi_2^2\eta_7}{4\xi_1\xi_3} - \frac{\eta_8}{4} + \frac{\xi_2\eta_8}{4\xi_1} - \frac{\xi_2\eta_8}{4\xi_3} + \frac{\xi_2^2\eta_8}{4\xi_1\xi_3}, \\
c_2 =& \frac{\xi_2\eta_2}{4\xi_1} - \frac{\xi_1\eta_2}{4\xi_3} + \frac{\xi_2\eta_2}{2\xi_3} + \frac{\xi_2^2\eta_2}{4\xi_1\xi_3} + \frac{\xi_2\eta_3}{4\xi_1} - \frac{\xi_1\eta_3}{4\xi_3} + \frac{\xi_2^2\eta_3}{4\xi_1\xi_3} + \frac{\eta_4}{2} - \frac{5\xi_2\eta_4}{4\xi_1} + \frac{\xi_1\xi_2\eta_4}{4\xi_3^2} \\
&- \frac{\xi_2^2\eta_4}{4\xi_3^2} - \frac{5\xi_2^3\eta_4}{8\xi_1\xi_3^2} + \frac{\xi_1\eta_4}{4\xi_3} - \frac{5\xi_2^2\eta_4}{4\xi_1\xi_3} - \frac{\xi_2\eta_5}{4\xi_1} + \frac{\xi_1\xi_2\eta_5}{4\xi_3^2} - \frac{\xi_2^3\eta_5}{8\xi_1\xi_3^2} + \frac{\xi_1\eta_5}{4\xi_3} - \frac{\xi_2^2\eta_5}{4\xi_1\xi_3} - \frac{\eta_7}{2} \\
&+ \frac{5\xi_2\eta_7}{4\xi_1} - \frac{\xi_1\eta_7}{4\xi_3} + \frac{5\xi_2^2\eta_7}{4\xi_1\xi_3} + \frac{\xi_2\eta_8}{4\xi_1} - \frac{\xi_1\eta_8}{4\xi_3} + \frac{\xi_2^2\eta_8}{4\xi_1\xi_3},
\end{aligned}$$

$$
\begin{aligned}
c_3 =& -\frac{\xi_2\eta_1}{4\xi_1} - \frac{\xi_2^2\eta_1}{2\xi_1^2} - \frac{\xi_2^2\eta_1}{8\xi_1\xi_3} - \frac{\xi_2^3\eta_1}{4\xi_1^2\xi_3} + \frac{\eta_2}{4} + \frac{3\xi_2\eta_2}{4\xi_1} - \frac{\xi_2^2\eta_2}{2\xi_1^2} - \frac{\xi_2\eta_2}{4\xi_3} + \frac{5\xi_2^2\eta_2}{8\xi_1\xi_3} - \frac{\xi_2^3\eta_2}{4\xi_1^2\xi_3} \\
& + \frac{\eta_3}{4} + \frac{\xi_2\eta_3}{2\xi_1} - \frac{\xi_2\eta_3}{4\xi_3} + \frac{\xi_2^2\eta_3}{2\xi_1\xi_3} - \frac{\eta_4}{2} - \frac{\xi_2\eta_4}{2\xi_1} + \frac{\xi_2^2\eta_4}{4\xi_3^2} - \frac{\xi_2^3\eta_4}{4\xi_1\xi_3^2} - \frac{\xi_2^2\eta_4}{2\xi_1\xi_3} - \frac{\eta_5}{2} \\
& - \frac{\xi_2\eta_5}{2\xi_1} + \frac{\xi_2^2\eta_5}{4\xi_3^2} - \frac{\xi_2^3\eta_5}{4\xi_1\xi_3^2} - \frac{\xi_2^2\eta_5}{2\xi_1\xi_3} + \frac{\eta_7}{2} + \frac{\xi_2\eta_7}{2\xi_1} + \frac{\xi_2^2\eta_7}{2\xi_1\xi_3} + \frac{\eta_8}{2} + \frac{\xi_2\eta_8}{2\xi_1} + \frac{\xi_2^2\eta_8}{2\xi_1\xi_3}, \\
c_4 =& -\frac{\xi_2^2\eta_1}{2\xi_1^2} - \frac{\xi_2^3\eta_1}{4\xi_1^2\xi_3} + \frac{\xi_2\eta_2}{\xi_1} - \frac{\xi_2^2\eta_2}{\xi_1^2} - \frac{\xi_1\eta_2}{4\xi_3} - \frac{\xi_2\eta_2}{2\xi_3} + \frac{\xi_2^2\eta_2}{\xi_1\xi_3} - \frac{\xi_2^3\eta_2}{2\xi_1^2\xi_3} + \frac{\xi_2\eta_3}{\xi_1} - \frac{\xi_1\eta_3}{4\xi_3} \\
& + \frac{3\xi_2^2\eta_3}{4\xi_1\xi_3} - \frac{\eta_4}{2} - \frac{\xi_2\eta_4}{\xi_1} + \frac{\xi_1\xi_2\eta_4}{4\xi_3^2} + \frac{\xi_2^2\eta_4}{4\xi_3^2} - \frac{\xi_2^3\eta_4}{2\xi_1\xi_3^2} + \frac{\xi_1\eta_4}{4\xi_3} - \frac{\xi_2^2\eta_4}{\xi_1\xi_3} - \frac{\xi_2\eta_5}{2\xi_1} + \frac{\xi_1\xi_2\eta_5}{4\xi_3^2} \\
& - \frac{\xi_2^3\eta_5}{4\xi_1\xi_3^2} + \frac{\xi_1\eta_5}{4\xi_3} - \frac{\xi_2^2\eta_5}{2\xi_1\xi_3} + \frac{\eta_7}{2} + \frac{\xi_2\eta_7}{\xi_1} - \frac{\xi_1\eta_7}{4\xi_3} + \frac{\xi_2^2\eta_7}{\xi_1\xi_3} + \frac{\xi_2\eta_8}{2\xi_1} - \frac{\xi_1\eta_8}{4\xi_3} + \frac{\xi_2^2\eta_8}{2\xi_1\xi_3}, \\
c_5 =& -\frac{\eta_1}{8} - \frac{\xi_2\eta_1}{8\xi_3} + \frac{3\xi_2\eta_2}{4\xi_1} - \frac{\xi_2^2\eta_2}{2\xi_1^2} - \frac{\xi_1\eta_2}{4\xi_3} + \frac{5\xi_2^2\eta_2}{8\xi_1\xi_3} - \frac{\xi_2^3\eta_2}{4\xi_1^2\xi_3} - \frac{\xi_2\eta_4}{2\xi_1} + \frac{\xi_1\xi_2\eta_4}{4\xi_3^2} \\
& - \frac{\xi_2^3\eta_4}{4\xi_1\xi_3^2} + \frac{\xi_1\eta_4}{4\xi_3} - \frac{\xi_2^2\eta_4}{2\xi_1\xi_3} + \frac{\xi_2\eta_7}{2\xi_1} - \frac{\xi_1\eta_7}{4\xi_3} + \frac{\xi_2^2\eta_7}{2\xi_1\xi_3}, \\
c_6 =& \frac{\eta_2}{2} + \frac{\xi_2\eta_2}{2\xi_1} + \frac{\xi_1\eta_2}{4\xi_3} + \frac{\xi_2^2\eta_2}{2\xi_1\xi_3} + \frac{\xi_1\eta_3}{4\xi_3} - \frac{\eta_4}{2} - \frac{\xi_2\eta_4}{2\xi_1} - \frac{\xi_1\xi_2\eta_4}{2\xi_3^2} - \frac{\xi_2^2\eta_4}{4\xi_3^2} - \frac{\xi_2^3\eta_4}{4\xi_1\xi_3^2} \\
& - \frac{\xi_1\eta_4}{2\xi_3} - \frac{\xi_2\eta_4}{2\xi_3} - \frac{\xi_2^2\eta_4}{2\xi_1\xi_3} + \frac{\eta_7}{2} + \frac{\xi_2\eta_7}{2\xi_1} + \frac{\xi_1\eta_7}{2\xi_3} + \frac{\xi_2\eta_7}{2\xi_3} + \frac{\xi_2^2\eta_7}{2\xi_1\xi_3}, \\
c_7 =& \frac{\xi_2\eta_1}{4\xi_3} + \frac{\xi_2\eta_2}{2\xi_1} - \frac{\xi_1\eta_2}{4\xi_3} + \frac{\xi_2^2\eta_2}{2\xi_1\xi_3} - \frac{\xi_2\eta_4}{2\xi_1} + \frac{\xi_1^2\eta_4}{8\xi_3^2} - \frac{\xi_2^2\eta_4}{2\xi_3^2} - \frac{\xi_2^3\eta_4}{4\xi_1\xi_3^2} + \frac{\xi_1\eta_4}{4\xi_3} - \frac{\xi_2\eta_4}{2\xi_3} \\
& - \frac{\xi_2^2\eta_4}{2\xi_1\xi_3} + \frac{\xi_1^2\eta_5}{8\xi_3^2} + \frac{\xi_2\eta_7}{2\xi_1} - \frac{\xi_1\eta_7}{4\xi_3} + \frac{\xi_2\eta_7}{2\xi_3} + \frac{\xi_2^2\eta_7}{2\xi_1\xi_3}, \\
c_8 =& \frac{\eta_1}{8} + \frac{\xi_2\eta_1}{8\xi_1} - \frac{\xi_2\eta_1}{8\xi_3} + \frac{\xi_2^2\eta_1}{8\xi_1\xi_3} + \frac{\xi_1\eta_2}{4\xi_3} - \frac{5\xi_1^2\eta_4}{32\xi_3^2} + \frac{\xi_1\xi_2\eta_4}{32\xi_3^2} - \frac{\xi_2^2\eta_4}{8\xi_3^2} - \frac{\xi_1\eta_4}{8\xi_3} - \frac{\xi_2\eta_4}{8\xi_3} \\
& - \frac{\xi_1^2\eta_5}{32\xi_3^2} + \frac{\xi_1\xi_2\eta_5}{32\xi_3^2} + \frac{\xi_1\eta_7}{8\xi_3} + \frac{\xi_2\eta_7}{8\xi_3}, \\
c_9 =& \frac{\xi_2\eta_1}{8\xi_1} + \frac{\xi_2^2\eta_1}{8\xi_1\xi_3} + \frac{\xi_1^2\eta_4}{16\xi_3^2} - \frac{3\xi_1\xi_2\eta_4}{32\xi_3^2} - \frac{\xi_2^2\eta_4}{8\xi_3^2} - \frac{\xi_2\eta_4}{8\xi_3} + \frac{\xi_1\xi_2\eta_5}{32\xi_3^2} + \frac{\xi_2\eta_7}{8\xi_3}, \\
c_{10} =& -\frac{\eta_1}{16} - \frac{\xi_2\eta_1}{8\xi_1} - \frac{\xi_2\eta_1}{16\xi_3} - \frac{\xi_2^2\eta_1}{8\xi_1\xi_3} + \frac{5\eta_2}{16} + \frac{\xi_2\eta_2}{8\xi_1} - \frac{\xi_2\eta_2}{16\xi_3} + \frac{\xi_2^2\eta_2}{8\xi_1\xi_3} + \frac{\xi_2\eta_3}{8\xi_3} + \frac{\xi_1\xi_2\eta_4}{8\xi_3^2} \\
& - \frac{\xi_2^2\eta_4}{8\xi_3^2} - \frac{\xi_1\eta_4}{8\xi_3} - \frac{\xi_2\eta_4}{8\xi_3} + \frac{\xi_1\xi_2\eta_5}{8\xi_3^2} - \frac{\xi_2^2\eta_5}{8\xi_3^2} - \frac{\xi_1\eta_5}{8\xi_3} - \frac{\xi_2\eta_5}{8\xi_3} + \frac{\xi_1\eta_7}{8\xi_3} + \frac{\xi_2\eta_7}{8\xi_3} \\
& + \frac{\xi_1\eta_8}{8\xi_3} + \frac{\xi_2\eta_8}{8\xi_3}, \\
c_{11} =& \frac{\eta_1}{8} - \frac{\xi_2\eta_1}{8\xi_3} - \frac{3\xi_1\eta_2}{8\xi_3} + \frac{\xi_2\eta_2}{4\xi_3} + \frac{\eta_3}{8} + \frac{\xi_2\eta_3}{4\xi_3} + \frac{\xi_1^2\eta_4}{8\xi_3^2} + \frac{\xi_1\xi_2\eta_4}{8\xi_3^2} - \frac{\xi_2^2\eta_4}{4\xi_3^2} - \frac{\xi_1\eta_4}{8\xi_3} \\
& - \frac{\xi_2\eta_4}{4\xi_3} + \frac{\xi_1^2\eta_5}{8\xi_3^2} - \frac{\xi_2^2\eta_5}{8\xi_3^2} + \frac{\xi_2\eta_5}{8\xi_3} + \frac{\xi_1\eta_7}{8\xi_3} + \frac{\xi_2\eta_7}{4\xi_3} + \frac{\xi_2\eta_8}{8\xi_3},
\end{aligned}
$$

$$c_{12} = \frac{\xi_2\eta_1}{8\xi_1} - \frac{3\xi_1\eta_1}{16\xi_3} + \frac{\xi_2^2\eta_1}{8\xi_1\xi_3} + \frac{\eta_2}{16} - \frac{\xi_2\eta_2}{8\xi_1} + \frac{3\xi_2\eta_2}{16\xi_3} - \frac{\xi_2^2\eta_2}{8\xi_1\xi_3} + \frac{\xi_1^2\eta_4}{8\xi_3^2} - \frac{\xi_2^2\eta_4}{8\xi_3^2} - \frac{\xi_2\eta_4}{8\xi_3} + \frac{\xi_2\eta_7}{8\xi_3}.$$

Appendix B Non-dimensional field equations

The full forms of the non-dimensional field equations (3.3) and (3.4) are given below:

$$\begin{aligned}
&(2\xi_2 + 2\xi_3)v_z + \xi_1 w_{zz} + 4\xi_3 w_s + s((2\xi_2 + 2\xi_3)v_{sz} + 4\xi_3 w_{ss}) \\
&+ \epsilon[(2\eta_2 + 2\eta_3 + 2\eta_7 + 2\eta_8)vv_z + (2\eta_2 + 2\eta_7)v_z w_z + 2\eta_2 v w_{zz} + \eta_1 w_z w_{zz} \\
&+ (4\eta_4 + 4\eta_5)v w_s + 4\eta_4 w_z w_s + s(\eta_4 v_z v_{zz} + (2\eta_2 + 2\eta_3 + 10\eta_7 + 2\eta_8)v_s v_z \\
&+ 2\eta_2 w_{zz} v_s + 2\eta_7 v_{zz} w_s + (20\eta_4 + 4\eta_5)v_s w_s + (2\eta_2 + 2\eta_3 + 2\eta_7 + 2\eta_8)v v_{sz} \\
&+ (2\eta_2 + 2\eta_7)w_s v_{sz} + 4\eta_7 v_z w_{sz} + 8\eta_4 w_s w_{sz} + (4\eta_4 + 4\eta_5)v w_{ss} + 4\eta_4 w_z w_{ss} \\
&+ s^2((4\eta_2 + 4\eta_7)v_s v_{sz} + 4\eta_7 v_z v_{ss} + 8\eta_4 w_s v_{ss} + 8\eta_4 v_s w_{ss})] + \epsilon^2[(\theta_2 + 3\theta_4 + \theta_{12} \\
&+ \theta_{13} + 2\theta_{15})v^2 v_z + (2\theta_3 + 2\theta_4 + 2\theta_{14} + 2\theta_{15})v v_z w_z + (\theta_2 + \theta_{12})v_z w_z^2 + (\theta_3 + \theta_4)v^2 w_{zz} \\
&+ 2\theta_2 v w_z w_{zz} + \frac{1}{2}\theta_1 w_z^2 w_{zz} + (2\theta_5 + 2\theta_6 + 4\theta_8)v^2 w_s + (4\theta_7 + 4\theta_8)v w_z w_s + 2\theta_5 w_z^2 w_s \\
&+ s((\frac{2}{3}\theta_{16} + \frac{1}{2}\theta_7 + \frac{1}{2}\theta_8)v_z^3 + (\theta_7 + \theta_8)v v_z v_{zz} + \theta_5 v_z w_z v_{zz} + \frac{1}{2}\theta_5 v_z^2 w_{zz} \\
&+ (10\theta_{12} + 2\theta_{13} + 12\theta_{15} + 2\theta_2 + 6\theta_4)v v_z v_s + (10\theta_{14} + 2\theta_{15} + 2\theta_3 + 2\theta_4)v_z w_z v_s \\
&+ (2\theta_3 + 2\theta_4)v w_{zz} v_s + 2\theta_2 w_z w_{zz} v_s + (2\theta_{14} + 2\theta_{15} + 4\theta_{17})v_z^2 w_s + (2\theta_{14} + 2\theta_{15})v v_{zz} w_s \\
&+ 2\theta_{12} w_z v_{zz} w_s + 2\theta_{12} v_z w_{zz} w_s + (20\theta_5 + 4\theta_6 + 24\theta_8)v v_s w_s + (20\theta_7 + 4\theta_8)w_z v_s w_s \\
&+ (8\theta_{16} + 2\theta_7 + 2\theta_8)v_z w_s^2 + 2\theta_5 w_{zz} w_s^2 + \frac{16}{3}\theta_9 w_s^3 + (\theta_{12} + \theta_{13} + 2\theta_{15} + \theta_2 + 3\theta_4)v^2 v_{sz} \\
&+ (2\theta_{14} + 2\theta_{15} + 2\theta_3 + 2\theta_4)v w_z v_{sz} + (\theta_{12} + \theta_2)w_z^2 v_{sz} + (4\theta_{14} + 4\theta_{15})v v_z w_{sz} + 2\theta_5 w_z^2 w_{ss} \\
&+ 4\theta_{12} v_z w_z w_{sz} + (8\theta_7 + 8\theta_8)v w_s w_{sz} + 8\theta_5 w_z w_s w_{sz} + (2\theta_5 + 2\theta_6 + 4\theta_8)v^2 w_{ss} \\
&+ (4\theta_7 + 4\theta_8)v w_z w_{ss}) + s^2(2\theta_7 v_z v_{zz} v_s + (16\theta_{12} + 4\theta_{15} + 2\theta_2 + 2\theta_4)v_z v_s^2 + 16\theta_7 v_s w_s w_{sz} \\
&+ 2\theta_3 w_{zz} v_s^2 + 4\theta_{14} v_{zz} v_s w_s + (\theta_{16} + \theta_7)v_z^2 v_{sz} + (4\theta_{12} + 4\theta_{15} + 4\theta_2 + 4\theta_4)v v_s v_{sz} \\
&+ (4\theta_{14} + 4\theta_3)w_z v_s v_{sz} + (4\theta_{14} + 4\theta_{17})v_z w_s v_{sz} + (4\theta_{16} + 4\theta_7)w_s^2 v_{sz} + 8\theta_{14} v_z v_s w_{sz}
\end{aligned}$$

$$
\begin{aligned}
&+(4\theta_{12}+4\theta_{15})vv_zv_{ss}+4\theta_{14}v_zw_zv_{ss}+(8\theta_5+8\theta_8)vw_sv_{ss}+8\theta_7w_zw_sv_{ss}+2\theta_{17}v_z^2w_{ss}\\
&+(8\theta_5+8\theta_8)vv_sw_{ss}+8\theta_7w_zv_sw_{ss}+8\theta_{16}v_zw_sw_{ss}+8\theta_9w_s^2w_{ss}+(32\theta_5+8\theta_8)v_s^2w_s)\\
&+s^3((4\theta_{12}+4\theta_2)v_s^2v_{sz}+8\theta_{12}v_zv_sv_{ss}+16\theta_5v_sw_sv_{zz}+8\theta_5v_s^2w_{ss})]=0,
\end{aligned}
\tag{B1}
$$

$$
\begin{aligned}
&\xi_3v_{zz}+8\xi_1v_s+(2\xi_2+2\xi_3)w_{sz}+4s\xi_1v_{ss}+\epsilon[(\frac{5}{2}\eta_4+\frac{1}{2}\eta_5)v_z^2+(\eta_4+\eta_5)vv_{zz}\\
&+\eta_4w_zv_{zz}+\eta_4v_zw_{zz}+(8\eta_1+8\eta_2)vv_s+8\eta_2w_zv_s+8\eta_7v_zw_s+2\eta_7w_{zz}w_s\\
&+(6\eta_4-2\eta_5)w_s^2+(2\eta_2+2\eta_3+2\eta_7+2\eta_8)vw_{sz}+(2\eta_2+2\eta_7)w_zw_{sz}+s(2\eta_4v_{zz}v_s\\
&+(14\eta_1+2\eta_2)v_s^2+4\eta_4v_zv_{sz}+8\eta_7w_sv_{sz}+(4\eta_2+4\eta_7)v_sw_{sz}+(4\eta_1+4\eta_2)vv_{ss}\\
&+4\eta_2w_zv_{ss}+4\eta_7v_zw_{ss}+8\eta_4w_sw_{ss})+8s^2\eta_1v_sv_{ss}]+\epsilon^2[(\frac{5}{2}\theta_5+\frac{1}{2}\theta_6+3\theta_8)vv_z^2\\
&+(\frac{5}{2}\theta_7+\frac{1}{2}\theta_8)v_z^2w_z+(\frac{1}{2}\theta_5+\frac{1}{2}\theta_6+\theta_8)v^2v_{zz}+(\theta_7+\theta_8)vw_zv_{zz}+\frac{1}{2}\theta_5w_z^2v_{zz}\\
&+(\theta_7+\theta_8)vv_zw_{zz}+\theta_5v_zw_zw_{zz}+(4\theta_1+8\theta_2+4\theta_3)v^2v_s+(8\theta_2+8\theta_4)vw_zv_s\\
&+4\theta_3w_z^2v_s+(8\theta_{12}+8\theta_{15})vv_zw_s+8\theta_{14}v_zw_zw_s+(2\theta_{14}+2\theta_{15})vw_{zz}w_s+2\theta_{12}w_zw_{zz}w_s\\
&+(6\theta_5-2\theta_6+4\theta_8)vw_s^2+(6\theta_7-2\theta_8)w_zw_s^2+(\theta_{12}+\theta_{13}+2\theta_{15}+\theta_2+3\theta_4)v^2w_{sz}\\
&+(2\theta_{14}+2\theta_{15}+2\theta_3+2\theta_4)vw_zw_{sz}+(\theta_{12}+\theta_2)w_z^2w_{sz}+s(\frac{1}{2}\theta_9v_z^2v_{zz}+(8\theta_5+2\theta 8)v_z^2v_s\\
&+(2\theta_5+2\theta_8)vv_{zz}v_s+2\theta_7w_zv_{zz}v_s+2\theta_7v_zw_{zz}v_s+(14\theta_1+16\theta_2+2\theta_3)vv_s^2\\
&+(14\theta_2+2\theta_4)w_zv_s^2+2\theta_{16}v_zv_{zz}w_s+(28\theta_{12}+4\theta_{15})v_zv_sw_s+4\theta_{14}w_{zz}v_sw_s\\
&+2\theta_{17}v_{zz}w_s^2+24\theta_5v_sw_s^2+(4\theta_5+4\theta_8)vv_zv_{sz}+4\theta_7v_zw_zv_{sz}+(8\theta_{12}+8\theta_{15})vw_sv_{sz}\\
&+8\theta_{14}w_zw_sv_{sz}+(\theta_{16}+\theta_7)v_z^2w_{sz}+(4\theta_{12}+4\theta_{15}+4\theta_2+4\theta_4)vv_sw_{sz}\\
&+(4\theta_{14}+4\theta_3)w_zv_sw_{sz}+(4\theta_{14}+4\theta_{17})v_zw_sw_{sz}+(4\theta_{16}+4\theta_7)w_s^2w_{sz}\\
&+(2\theta_1+4\theta_2+2\theta_3)v^2v_{ss}+(4\theta_2+4\theta_4)vw_zv_{ss}+2\theta_3w_z^2v_{ss}+(4\theta_{12}+4\theta_{15})vv_zw_{ss}\\
&+4\theta_{14}v_zw_zw_{ss}+(8\theta_5+8\theta_8)vw_sw_{ss}+8\theta_7w_zw_sw_{ss})+s^2(2\theta_5v_{zz}v_s^2+(\frac{40}{3}\theta_1+\frac{8}{3}\theta_2)v_s^3\\
&+8\theta_5v_zv_sv_{sz}+16\theta_{12}v_sw_sv_{sz}+(4\theta_{12}+4\theta_2)v_s^2w_{sz}+2\theta_5v_z^2v_{ss}+(8\theta_1+8\theta_2)vv_sv_{ss}\\
&+8\theta_2w_zv_sv_{ss}+8\theta_{12}v_zw_sv_{ss}+8\theta_5w_s^2v_{ss}+8\theta_{12}v_zv_sw_{ss}+16\theta_5v_sw_sw_{ss})\\
&+8s^3\theta_1v_s^2v_{ss}]=0.
\end{aligned}
\tag{B2}
$$

Appendix C

The full forms of the terms H_1-H_7 in equations (4.4)-(4.8) are given below:

$$
\begin{aligned}
H_1 =&(2\theta_5 + 2\theta_6 + 4\theta_8)V_0^2W_1 + (\theta_{12} + \theta_{13} + 2\theta_{15} + \theta_2 + 3\theta_4)V_0^2V_{0z}\\
&+ (4\theta_7 + 4\theta_8)V_0W_1W_{0z} + (2\theta_{14} + 2\theta_{15} + 2\theta_3 + 2\theta_4)V_0V_{0z}W_{0z} + 2\theta_5W_1W_{0z}^2\\
&+ (\theta_{12} + \theta_2)V_{0z}W_{0z}^2 + (\theta_3 + \theta_4)V_0^2W_{0zz} + 2\theta_2V_0W_{0z}W_{0zz} + \frac{1}{2}\theta_1W_{0z}^2W_{0zz},\\
H_2 =&(24\theta_5 + 8\theta_6 + 32\theta_8)V_0V_1W_1 + \frac{16}{3}\theta_9W_1^3 + (8\theta_5 + 8\theta_6 + 16\theta_8)V_0^2W_2\\
&+ (12\theta_{12} + 4\theta_{13} + 16\theta_{15} + 4\theta_2 + 12\theta_4)V_0V_1V_{0z} + (8\theta_{16} + 2\theta_7 + 2\theta_8)W_1^2V_{0z}\\
&+ (2\theta_{14} + 2\theta_{15} + 4\theta_{17})W_1V_{0z}^2 + (\frac{2}{3}\theta_{16} + \frac{1}{2}\theta_7 + \frac{1}{2}\theta_8)V_{0z}^3 + 8\theta_5W_2W_{0z}^2\\
&+ (2\theta_{12} + 2\theta_{13} + 4\theta_{15} + 2\theta_2 + 6\theta_4)V_0^2V_{1z} + (24\theta_7 + 8\theta_8)V_1W_1W_{0z}\\
&+ (16\theta_7 + 16\theta_8)V_0W_2W_{0z} + (12\theta_{14} + 4\theta_{15} + 4\theta_3 + 4\theta_4)V_1V_{0z}W_{0z} + (4\theta_{14} + 4\theta_{15}\\
&+ 4\theta_3 + 4\theta_4)V_0V_{1z}W_{0z} + (12\theta_{12} + 2\theta_2)V_{1z}W_{0z}^2 + (12\theta_7 + 12\theta_8)V_0W_1W_{1z}\\
&+ (6\theta_{14} + 6\theta_{15} + 2\theta_3 + 2\theta_4)V_0V_{0z}W_{1z} + 12\theta_5W_1W_{0z}W_{1z} + (6\theta_{12} + 2\theta_2)V_{0z}W_{0z}W_{1z}\\
&+ (2\theta_{14} + 2\theta_{15})V_0W_1V_{0zz} + (\theta_7 + \theta_8)V_0V_{0z}V_{0zz} + 2\theta_{12}W_1W_{0z}V_{0zz} + \theta_5V_{0z}W_{0z}V_{0zz}\\
&+ (4\theta_3 + 4\theta_4)V_0V_1W_{0zz} + 2\theta_5W_1^2W_{0zz} + 2\theta_{12}W_1V_{0z}W_{0zz} + \frac{1}{2}\theta_5V_{0z}^2W_{0zz}\\
&+ 4\theta_2V_1W_{0z}W_{0zz} + 2\theta_2V_0W_{1z}W_{0zz} + \theta_1W_{0z}W_{1z}W_{0zz} + (\theta_3 + \theta_4)V_0^2W_{1zz}\\
&+ 2\theta_2V_0W_{0z}W_{1zz} + \frac{1}{2}\theta_1W_{0z}^2W_{1zz},\\
H_3 =&(4\theta_1 + 8\theta_2 + 4\theta_3)V_0^2V_1 + (6\theta_5 - 2\theta_6 + 4\theta_8)V_0W_1^2 + (8\theta_{12} + 8\theta_{15})W_1V_{0z}\\
&+ (\frac{5}{2}\theta_5 + \frac{1}{2}\theta_6 + 3\theta_8)V_0V_{0z}^2 + (8\theta_2 + 8\theta_4)V_0V_1W_{0z} + (6\theta_7 - 2\theta_8)W_1^2W_{0z}\\
&+ 8\theta_{14}W_1V_{0z}W_{0z} + (\frac{5}{2}\theta_7 + \frac{1}{2}\theta_8)V_{0z}^2W_{0z} + 4\theta_3V_1W_{0z}^2 + (\theta_{12} + \theta_{13}\\
&+ 2\theta_{15} + \theta_2 + 3\theta_4)V_0^2W_{1z} + (2\theta_{14} + 2\theta_{15} + 2\theta_3 + 2\theta_4)V_0W_{0z}W_{1z}\\
&+ (\theta_{12} + \theta_2)W_{0z}^2W_{1z} + (\frac{1}{2}\theta_5 + \frac{1}{2}\theta_6 + \theta_8)V_0^2V_{0zz} + (\theta_7 + \theta_8)V_0W_{0z}V_{0zz}
\end{aligned}
$$

$$
\begin{aligned}
&+\frac{1}{2}\theta_5 W_{0z}^2 V_{0zz}+(2\theta_{14}+2\theta_{15})V_0W_1W_{0zz}+(\theta_7+\theta_8)V_0V_{0z}W_{0zz}\\
&+2\theta_{12}W_1W_{0z}W_{0zz}+\theta_5V_{0z}W_{0z}W_{0zz},\\
H_4=&(\frac{1}{6}\theta_1+\frac{2}{3}\theta_2+\frac{1}{2}\theta_3)V_0^3+(\frac{1}{2}\theta_2+\frac{3}{2}\theta_4)V_0^2W_{0z}+(\frac{1}{2}\theta_3+\frac{1}{2}\theta_4)V_0W_{0z}^2+\frac{1}{6}\theta_2W_{0z}^3,\\
H_5=&(3\eta_1+5\eta_2)V_0V_1+2\eta_4W_1^2+2\eta_7W_1V_{0z}+\frac{1}{2}\eta_4V_{0z}^2+(3\eta_2+\eta_3)V_1W_{0z}\\
&+(\eta_2+\eta_3)V_0W_{1z}+\eta_2W_{0z}W_{1z},\\
H_6=&(\theta_5+\theta_6+2\theta_8)V_0^2W_1+(\frac{1}{2}\theta_{12}+\frac{1}{2}\theta_{13}+\theta_{15})V_0^2V_{0z}+(2\theta_7+2\theta_8)V_0W_1W_{0z}\\
&+(\theta_{14}+\theta_{15})V_0V_{0z}W_{0z}+\theta_5W_1W_{0z}^2+\frac{1}{2}\theta_{12}V_{0z}W_{0z}^2,\\
H_7=&(6\eta_4+2\eta_5)V_1W_1+(4\eta_4+4\eta_5)V_0W_2+(3\eta_7+\eta_8)V_1V_{0z}+(\eta_7+\eta_8)V_0V_{1z}\\
&+4\eta_4W_2W_{0z}+\eta_7V_{1z}W_{0z}+2\eta_4W_1W_{1z}+\eta_7V_{0z}W_{1z}.
\end{aligned}
$$

References

[1] Abeyaratne, R., Bhattacharya, K., Knowles, J.K., 2001. Strain-energy functions with multiple local minima: modeling phase transformations using finite thermoelasticity. In: Fu, Y., Ogden, R. (Eds.), Nonlinear elasticity: theory and applications, Cambridge: Cambridge University Press, pp. 433-490.

[2] Aifantis, E.C., Serrin, J.B., 1983. Equilibrium solutions in the mechanical theory of fluid microstructures, J. Colloid Inter. Sci. 96, 530-547.

[3] Ball, J.M., James, R.D., 1992. Proposed experimental tests of a theory of fine microstructure and the two well problem, Phil. Trans. R. Soc. A 338, 389-450.

[4] Cai, Z.X., Dai, H.H., 2006. Phase transitions in a slender cylinder composed of an incompressible elastic material. II. Analytical solutions for two boundary-value problems, Proc. R. Soc. Lond. Ser. A Math. Phys. Eng. Sci. 462, 419-438.

[5] Chang, B.C., Shaw, J.A., Iadicola, M.A., 2006. Thermodynamics of shape memory alloy wire: modeling, experiments, and application, Continuum Mech. Thermodyn. 18, 83-118.

[6] Coleman, B.D., 1983. Necking and drawing in polymeric fibers under tension, Arch. Ration. Mech. 83, 47-58.

[7] Dai, H.H., Huo, Y., 2002. Asymptotically approximate model equations for nonlinear dispersive waves in incompressible elastic rods, Acta Mech. 157, 97-112.

[8] Dai, H.H., Fan, X.J., 2004. Asymptotically approximate model equations for weakly nonlinear long waves in compressible elastic rods and their comparisons with other simplified model equations, Math. Mech. Solids 9, 61-79.

[9] Dai, H.H., Cai, Z.X., 2006. Phase transitions in a slender cylinder composed of an incompressible elastic material. I. Asymptotic model equation, Proc. R. Soc. Lond. Ser. A Math. Phys. Eng. Sci. 462, 75-95.

[10] Ericksen, J.L., 1975. Equilibrium bars, J. Elast. 5, 191-201.

[11] Favier, D., Liu, Y., Orgeas, L., Rio, G., 2001. Mechanical instability of NiTi in tension, compression and shear. In: Sun, Q.P. (Eds.), Proc. IUTAM symp. on Mechanics of Martensitic Phase Transformation in Solids, Boston; Kluwer Academic Publishers, pp. 205-212.

[12] Fu, Y.B., Ogden, R.W., 1999. Nonlindar stability analysis of pre-stressed elastic bodies, Continuum Mech. Thermodyn. 11, 141-172.

[13] Li, Z.Q., Sun, Q.P., 2002. The initiation and growth of macroscopic martensite band in nanograined NiTi microtube under tension, Inter J. Plast. 18, 1481-1498.

[14] Pelton, A., Hodgson, D., Russell, S., Duerig, T., (eds) 1997 Proc. Second Int. Conf. on Shape Memory Superelastic Technologies (SMST-97), California, 2-6 March 1997. Los Angeles: SMST Publications.

[15] Shaw, J.A., 2002. A thermomechanical model for a 1-D shape memory alloy wire with propagating instabilities, Inter. J. Solids and Structures 39, 1275-1305.

[16] Shaw, J.A., Kyriakides, S., 1995. Thermomechanical aspects of NiTi, J. Mech. Phys. Solids 47, 1243-1281.

[17] Shaw, J.A., Kyriakides, S., 1997. On the nucleation and propagation of phase transformation fronts in a NiTi alloy, Acta Mater. 45, 683-700.

[18] Shaw, J.A., Kyriakides, S., 1998. Initiation and propagation of localized deformation in elasto-plastic strips under uniaxial tension, Inter. J. Plasticity 13, 837-871.

[19] Sun, Q.P., Li, Z.Q., Tse, Ken K.K., 2000. On superelastic deformation of NiTi shape memory alloy micro-tubes and wires–band nucleation and propagation. In: Gabbert U., Tzou H.s. (Eds.), Proc. IUTAM Symp. on Smart Structures and Structure Systems, Magdeburg, Germany: Kluwer Academic Publishers, pp. 1-8.

[20] Tong, P., Lam, C.C., Sun, Q.P., 2001. Phase transformation of thin wires in tension. In: Sun Q.P. (Eds.), Proc. IUTAM Symp. on Mechanics of Martensitic Phase Transformation in Solids, Hong Kong, 11-15 June 2001, Boston: Kluwer Academic Publishers, pp. 221-232.

[21] Triantafyllidis, N., Aifantis, E.C., 1986. A gradient approach to localization of deformation. 1. hyperelastic materials, J. Elasticity 16, 225-237.

[22] Trunskinovsky, L.M., 1982. Equilibrium interface boundaries, Sov. Phys. Dokl. 27, 551-553.

[23] Trunskinovsky, L.M., 1985. Structure of an isothermal phase discontinuity, Sov. Phys. Dokl. 30, 945-948.

[24] Tse, Ken K.K., Sun, Q.P., 2000. Some deformation features of polycrystalline superelastic NiTi shape memory alloy thin strips and wires under tension, Key Eng. Mat. 177-180, 455-460.